Safety-Critical Geometric Control for Systems on Manifolds Subject to Time-Varying Constraints

Guofan Wu and Koushil Sreenath

***Abstract*—We address the safety-critical control problem for systems whose dynamics evolve on manifolds using the concepts of control Lyapunov functions (CLFs) and control Barrier functions (CBFs). We first extend the concepts of CLFs and CBFs from Cartesian spaces to manifolds, resulting in geometric CLFs and CBFs. We then formulate a state-dependent online quadratic program (QP) that imposes the constraints of the geometric CLF and geometric CBF to compute the control input. The resulting geometric CBF-CLF-QP controller trades-off between tracking stability and critical safety. We test the controller's performance, with both time invariant and time-varying safety constraints, on simple mechanical systems such as, a 3D moving point mass, a spherical pendulum, and a 3D pendulum.**

***Keywords*—Geometric Control Lyapunov Function, Geometric Control Barrier Function, Time-varying Safety Critical Control.**

I. Introduction

EVERY robotic system has inherent constraints that need to be explicitly considered both in the design as well as implementation of controllers. These constraints could either be (a) imposed by limits of physical hardware systems, such as work-space constraints, joint position and velocity constraints, and input constraints; or (b) imposed by the controller for safe operation of the system, such as collision constraints, contact force constraints, range constraints, etc. These constraints typically manifest themselves as a combination of constraints on the inputs and states, and their enforcement becomes critically necessary for maintaining safety of the system.

Designing controllers that provide guarantees of enforcing safety-critical constraints is challenging. Further adding to the challenge is the fact that a significant number of robotic systems have dynamics that evolve on non-Euclidean spaces, whose configuration spaces are nonlinear manifolds. Most control design is carried out on local parametrizations of these nonlinear spaces, resulting in local results of stability and local constraint enforcement. Designing controllers directly on nonlinear manifolds to obtain global results of stability while enforcing constraints globally is challenging. Complicating matters even further is the fact that several of these safety-critical constraints are typically time-varying, presenting further challenges for control design.

G. Wu and K. Sreenath are with the Department of Mechanical Engineering, Carnegie Mellon University, Pittsburgh, PA 15213, email: {gwu,koushils}@andrew.cmu.edu.

This work is supported in part by the Google Faculty Research Award and in part by NSF grants IIS-1464337, CMMI-1538869, IIS-1526515.

A. Background

Over the past few decades, there have been several approaches towards solving the constrained control problem. Model predictive control (MPC) is a popular technique for constrained control problems that solves an online optimal control problem over a finite-horizon to handle input and state constraints in control design [10], [36], [33], with sufficient conditions for the stability presented in [23], [13]. However, MPC performance is determined by the size of the finite-horizon and the cost function for optimization, and choosing good candidates for these is challenging. Moreover, for high-dimensional systems with fast dynamics, solving a nonlinear programming problem at real-time speeds is not always feasible leading to latency issues that could lead to instability. Typical solutions to this involve simplifying the dynamics by considering a linear approximation.

Another approach to address constraints point-wise in time is to adjust the reference command using a pre-filter called reference governor [5]. However this typically requires online forward integration of the dynamics which is computationally expensive. Recent results in reduced-order reference governors [14] decompose the states into slow and fast dynamics and implement the reference governor based only on the slow states variables thereby reducing computational complexity, however, this comes at the cost of a smaller domain of attraction.

The safety-critical control problem has also been addressed through reachability analysis, wherein an unsafe region is propagated backwards in time based on a worst case analysis with model uncertainty considered as a two-player differential game [4], [22], [24], [1]. The evolving dynamics of this unsafe region is determined by a time-invariant Hamilton-Jacobi-Issacs (HJI) partial differential equation [22]. While the method of reachability analysis provides formal guarantees, its computationally expensive and does not scale well for high-dimensional systems with fast dynamics.

Motivated by the idea of forward invariance in stability theory, the concept of barrier functions (BF) has been established to realize safety-critical control [27], [37], [32], [31], [17], [16], wherein the unsafe set is outside a level set of the barrier function. Logarithmic barrier functions have also been considered in [21], [32] to handle input and output constraints, alongside safety constraints. Barrier functions have also been used to re-target the pose of satellites subject to cone inclusion and exclusion constraints [34], [16], [17]. Barrier functions have also been added to the objective functions to handle constrained MPC problems [36]. However, the concept of the barrier function considered here is limited since the imposed condition, on the time-derivative of the barrier function being non-negative, does not allow the state to transverse the

boundary of a level set of the barrier function. This results in an extremely conservative trajectory for the corresponding closed-loop system, even when the system state is far away from the unsafe region. Furthermore, finding a barrier function for a particular safe set is challenging.

The search for a barrier function with desirable properties on its time-derivative is simplified by the introduction of the concept of a control Barrier function (CBF), where the control inputs explicitly appear in the derivative of the barrier function [35]. Furthermore, to alleviate the conservative condition of the time-derivative of the barrier function being non-negative, [3] relaxes and proposes a new condition for the time-derivative of the barrier function to be negative while still guaranteeing the enforcement of the safety constraint. Similar to the concept of Control Lyapunov Function (CLF) in [29], [9], we are able to generate the control input which can account for the safety constraints through CBF-based optimization. [28] proposes the concept of Control Lyapunov Barrier Function (CLBF) which accounts for both safety constraints and tracking goal at the same time. [3] imposes the conditions of CLF and CBF separately as the constraints of a state-dependent quadratic programming (QP) through relaxation of the CLF condition allowing the reference trajectory to be tracked to be unsafe.

Furthermore, several typical mechanical systems have dynamics that evolve on non-Euclidean manifolds. Traditional dynamical models and controllers for such systems are constructed using local parametrizations, such as Euler angles, resulting in dynamics with singularities and controllers that are not valid globally [8]. To circumvent this dilemma, geometric control methods have been introduced to obtain almost-global controllers on manifolds [7], [19], [18], [20], [30]. Geometric controllers have been widely applied to fully actuated mechanical systems [7] and even underactuated system such as quadrotors [19], [20], [30]. However, these geometric controllers typically do not take into account input, state, or safety-critical constraints. Recent results in [15], [12] address geometric constraints on SO(3) using geometric reference governors and model predictive control. However, these methods require the discretization of the system and variation integration of the discrete dynamics, which are hard for high-dimensional or coupled nonlinear systems.

Having presented a brief overview of prior related work, we next tabulate the main contributions of our paper.

B. Contributions

Our paper is inspired by the recent work in CLFs and CBFs [3], [9], [2], [26] and builds off our preliminary results in [38]. The control architecture is based on a state-dependent online QP that enforces constraints of both CLFs and CBFs to make a trade-off between safety constraints and tracking goal. The major contributions of this paper are listed below:

- We extend the concept of CBFs to general Riemannian manifolds using coordinate-free formulations for the dynamics on manifolds and associated configuration errors and transport maps.
- The concept of a time-varying CBF is introduced for fully actuated, simple mechanical systems to allow enforcing time-varying safety constraints on Riemannian manifolds.
- We formulate a general method to construct CBF candidates based on time-varying safety regions in the configuration space, which result in geometric safety constraints with relative-degree 2.
- A geometric CBF-CLF-QP based controller is proposed to realize safety-critical trajectory tracking for fully-actuated simple mechanical systems at real-time speeds. Numerical validations are presented for the following three systems: a 3D-moving point mass, a spherical pendulum, and a 3D pendulum, with both time-invariant and time-varying safety constraints. The corresponding configuration spaces are $\mathbb{R}^3, \mathbb{S}^2, SO(3)$, ranging from flat Cartesian space to non-flat Lie group.

C. Organization

The remainder of this paper is organized as follows: Section II introduces the necessary concepts about CLF, CBF and geometric control. Section III describes a general control design method on simple mechanical systems whose configuration space is Riemann manifold. Note that the method provided here handles both the time-invariant and time-varying constraints. Section IV, VI and V present simulation results of this control method on three typical systems mentioned previously. Section VII summarizes the overall content.

II. Mathematical Preliminary

This section gives a detailed introduction on the relevant concepts in geometric control. Basic knowledge of differential geometry is assumed. Some intuitive examples are provided to help better understand these concepts. We refer to [11] for more details on differential geometry, [7] for more details on geometric control, and [2], [3] for a more details on control Lyapunov and control Barrier functions. Table I summarizes all the symbols used in this paper.

A. Fundamentals of Geometric Control

Given a mechanical system which evolves on a sufficiently smooth manifold M, we denote its configuration variable as q, the tangent space at q as T_qM and the tangent bundle as $TM = \cup T_qM$. Then the state space representation of this system is given by $(q, \dot{q}) \in TM$.

Further, a vector field is a mapping from each point $q \in M$ to a vector in the corresponding T_qM. While, an one form $\omega : T_qM \to \mathbb{R}$ defines a mapping from the tangent space at each point $q \in M$ to the real number. A common one form is *the differential* of a smooth function $f : M \to \mathbb{R}$ given by

$$\langle df, X \rangle_q = \lim_{t \to 0} \frac{f(\alpha(t)) - f(q)}{t},$$

where the curve $\alpha : [-1, 1] \to M$ satisfies $\alpha(0) = q \in M, \alpha'(0) = X \in T_qM$.

Suppose we define a smooth function on the unit sphere $\mathbb{S}^2 \subset \mathbb{R}^3$ as $f(q) = q \cdot n,\ q \in \mathbb{S}^2$. Then, from multi-variate calculus, its differential with a tangent vector $\dot{q} \in T_qM$ is given

TABLE I: NOMENCLATURE

Riemannian Geometry Concepts	
M	A Riemannian manifold representing configuration space.
m	The dimension of M
T_qM	The tangent space at the point $q \in M$.
T_q^*M	The cotangent space at the point $q \in M$.
TM	The tangent bundle of M representing state space as $\cup_{q\in M} T_qM$.
T^*M	The cotangent bundle of M defined as $\cup_{q\in M} T_q^*M$.
d_ig	An one-form in M representing the differential of g with respect to the i^{th} argument where $i \in \{1,2\}$.
d_id_jg	A two form in M which is the exterior derivative of d_jg with respect to the i^{th} argument where $i,j \in \{1,2\}$.
X, Y	Smooth vector fields defined on M.
$\langle d_ig, X\rangle_q$	The value of one-form dg_i of the vector X at point q.
$\langle\!\langle \cdot,\cdot \rangle\!\rangle_q$	A Riemannian metric which introduces an inner product to the tangent space T_qM at each $q \in M$.
$\nabla_X Y$	A Riemannian connection of X, Y which is uniquely determined by the Riemannian metric $\langle\!\langle \cdot,\cdot \rangle\!\rangle_q$.
Geometric Control Concepts	
M_q	The inertia tensor of a mechanical systems which maps from T_qM to T_q^*M.
$\langle\!\langle \dot{q}_1, \dot{q}_2 \rangle\!\rangle_q$	A Riemannian metric induced by the inertia M_q, i.e, $\langle\!\langle \dot{q}_1, \dot{q}_2 \rangle\!\rangle = \langle M_q\dot{q}_1, \dot{q}_2\rangle$, which is also called the inertia metric.
$\nabla_{\dot{q}}\dot{q}$	The acceleration term on M defined by the inertia metric.
$\Psi(q, q_d)$	The configuration error of manifold M.
e_q	The position error which is the differential of Ψ as $d_1\Psi$.
$\mathscr{T}_{q,q_d}$	The transport map which maps between tangent spaces of T_qM and $T_{q_d}M$.
$e_{\dot{q}}$	The velocity error which is a tangent vector in T_qM.
V_q	The potential function of a fully actuated simple mechanical system.
F_i	The external forces treated as a set of independent one-forms.
u_i	The i^{th} control input.
u	The control input vector defined as $[u_1, u_2, \cdots, u_m]^T$.
CLF and CBF Relevant Concepts	
k	The number of safety constraints given.
$g_i(t,q)$	A smooth function in $[0,\infty) \times M$ which defines a time-varying region in M.
$\mathcal{B}_{i,t}$	The time-varying safety region $\{q \in M : g_i(q) \geq 0\}$ in the configuration space.
$h_i(t,q,\dot{q})$	A smooth function in $[0,\infty) \times TM$ which is constructed based on g_i to enforce safety.
$\mathcal{C}_{i,t}$	The expanded safety region $\{(q,\dot{q}) \in TM : h_i(q) \geq 0\}$ in the state space.
$B_i(h_i)$	Time-varying geometric Control Barrier Function for the region $\mathcal{C}_i$.
$\mathcal{D}_{i,t}^B$	The singularity set with respect to the CBF B_i.
$V(t,q,\dot{q})$	Time-varying geometric Control Lyapunov Function for the reference $(q_d, \dot{q}_d)$.
$\mathcal{D}_t^V$	The singularity set with respect to the CLF V.

by $\langle df, \dot{q}\rangle_q = \dot{q}\cdot n$. Here we denote the differential of f as df and the value of the one form with tangent vector $\dot{q}$ at point q as $\langle \omega, \dot{q}\rangle_q$. Based on the notion of the one form, we are able to define a two form which is the exterior derivative of the one form. Similarly, we are able to get a two form from the differential of a function, which reflects the second order derivative of this function on a manifold. In particular, when a smooth function $f : M_1 \times M_2 \to \mathbb{R}$ is multivariate, we will denote its second order differential as:

$$d_id_jf = d_i(d_jf), \quad i,j \in \{1,2\} \tag{1}$$

where the first d_i is the exterior derivative of d_jf with respect to M_i.

Since mechanical systems are governed by Newton's law whose dynamics are represented as second order differential equations, we need a way to describe how $\dot{q}$ will evolve along the system trajectory, namely the acceleration term on a manifold. This requires the introduction of the notions of a Riemannian metric and a Riemannian connection. A Riemannian metric $\langle\!\langle \cdot,\cdot \rangle\!\rangle_q : T_qM \times T_qM \to \mathbb{R}$ is an inner product, defined on the tangent space T_qM, which changes smoothly as the tangent space is shifted from one point to another. Through this metric, every linear functional of the tangent space T_qM could be uniquely identified with an element in T_qM by the Riesz representation theorem. Intuitively, due to this metric, we can treat every vector in T_qM as *either a tangent vector or a linear functional.* We denote this linear functional space of T_qM as T_q^*M.

For example, consider a point mass with mass $M_q > 0$ in $M = \mathbb{R}^3$, then a candidate metric could be given as

$$\langle\!\langle \dot{q}_1, \dot{q}_2 \rangle\!\rangle_q = (M_q\dot{q}_1)\cdot\dot{q}_2, \quad \dot{q}_1, \dot{q}_2 \in T_qM.$$

From another perspective, the mass M_q actually maps a vector in T_qM to a linear functional in T_q^*M. Based on this metric, we are able to generate a Riemannian connection which is *compatible with it and torsion-free*. Intuitively, given two smooth vector fields X, Y, the connection $\nabla_X Y$ in M describes how the vector of Y at q would change if we move the point q along the direction of X. Given a Riemannian metric, a torsion-free, compatible connection could be uniquely determined, which we call the Riemannian connection.

***Remark* 1.** *For simplicity of notation, we will drop the explicit dependence of $\langle\!\langle \cdot,\cdot \rangle\!\rangle_q$ on $q \in M$ by dropping the subscript q to obtain $\langle\!\langle \cdot,\cdot \rangle\!\rangle$, with the expectation that the tangent vectors provides this information.*

Now we are able to describe a simple, fully actuated mechanical system and the corresponding geometric control law. If the configuration manifold M admits the following structure:

1) The total inertia represented by a metric $M_q : T_qM \to T_q^*M$ which represents the kinetic energy by $\langle\!\langle \dot{q}, \dot{q} \rangle\!\rangle = \langle M_q\dot{q}, \dot{q}\rangle$.
2) A connection ∇ which is compatible with M_q that serves to describe how a tangent vector or the velocity $\dot{q}$ changes along the manifold M.

3) A collection of one forms $F_i : T_qM \to \mathbb{R}$ representing the external force applied on the system, where $i \in \{1, 2, \cdots, m\}$. The span of these one forms is the entire cotangent space T_q^*M at each point q.
4) A smooth function $V_q : M \to \mathbb{R}$ describing the potential energy.
5) A configuration error $\Psi : M \times M \to [0, \infty)$ that serves as a measure of distance between the two points $q, q_d \in M$. We also require $\Psi(q, q_d)$ to be quadratic as defined in [7]. Denote the differential of the configuration error with respect to the i^{th} argument as $d_i\Psi$ $(i = 1, 2)$, and define the position error as $e_q = d_1\Psi$.
6) A transport map $\mathscr{T}_{(q,q_d)} : T_{q_d}M \to T_qM$ which maps a tangent vector at q_d to one at q with the compatible condition,

$$d_2\Psi = -\mathscr{T}^*_{(q,q_d)} d_1\Psi, \tag{2}$$

where $\mathscr{T}^*_{(q,q_d)}$ is the dual map of $\mathscr{T}_{(q,q_d)}$. In this way, we are able to compare tangent vectors in different tangent spaces as

$$e_{\dot{q}} = \dot{q} - \mathscr{T}_{(q,q_d)}\dot{q}_d.$$

Then, a system evolving on M with the above structure is called a simple mechanical system with dynamics given by [6],

$$\nabla_{\dot{q}}\dot{q} = M_q^{-1}(-dV_q(q) + \sum_{i=1}^{m} F_i(q, \dot{q})u_i), \tag{3}$$

where $u_i \in \mathbb{R}$.

For this type of system, a general PD-type feedback law could be set up which guarantees *exponential stability*. In order to track a dynamically feasible smooth reference $q_d(t) : [0, \infty) \to M$, a geometric control input could be expressed as

$$u = \underbrace{u_{ff}}_{\text{feedforward term}} + \underbrace{u_{fb}}_{\text{feedback term}},$$

where u_{fb} is a linear combination of the position and velocity errors, e_q and $e_{\dot{q}}$, and serves as a generalization of a PD control on the manifold M.

To get an exponentially stable controller, a general Lyapunov function candidate V for the *closed-loop system* could be expressed as:

$$V = \alpha\Psi(q, q_d) + \frac{1}{2}\langle\!\langle e_{\dot{q}}, e_{\dot{q}} \rangle\!\rangle + \varepsilon\langle e_q, e_{\dot{q}} \rangle, \tag{4}$$

where the value of ε and α are specifically chosen to make V *locally* quadratic in terms of the error $e_q, e_{\dot{q}}$.

For use later, we also define the hat map $\wedge : \mathbb{R}^3 \to \mathfrak{so}(3)$ as a bijective mapping from a three dimensional vector to a skew symmetric matrix as:

$$\hat{x} = \begin{bmatrix} 0 & -x_3 & x_2 \\ x_3 & 0 & -x_1 \\ -x_2 & x_1 & 0 \end{bmatrix},$$

where $x = [x_1, x_2, x_3]^T$ and the vee map $\vee : \mathfrak{so}(3) \to \mathbb{R}^3$ as the inverse of hat map.

B. Time-varying Exponentially Stabilizing Control Lyapunov Function (CLF)

In the sections below, we will introduce the concepts of control Lyapunov functions (CLFs) and control Barrier functions (CBFs). Though originally introduced for systems in Cartesian spaces, these concepts have been generalized to the case of simple mechanical systems (3) on manifolds, as studied in [38]. Consider a control affine system in $\mathbb{R}^n$ of the form,

$$\dot{x} = f(x) + g(x)u, \qquad x(t_0) = x_0, \tag{5}$$

where $x \in \mathbb{R}^n$ and $u \in \mathbb{R}^m$.

For system (5), a continuously differentiable function $V : [0, \infty) \times \mathbb{R}^n \to \mathbb{R}$ is called Exponentially Stabilizing Lyapunov Function (ES-CLF) if there exist constants $c_1, c_2, \eta > 0$ such that,

$$c_1\|x\|^2 \le V(t, x) \le c_2\|x\|^2,$$
$$\inf_{u \in \mathbb{R}^m} \{\frac{\partial V}{\partial t} + L_fV + L_gVu + \eta V\} \le 0,$$

holds for every $(t, x) \in [0, \infty) \times \mathbb{R}^n$ where $L_fV = \frac{\partial V}{\partial x} f$, $L_gV = \frac{\partial V}{\partial x} g$ are the Lie derivatives of V with respect to f and g.

***Remark* 2.** *CLFs give a qualitative analysis of the stability of the origin. If such a function exists, we could determine the control input analytically through the Sontag control or the min-norm control, or directly through a state-based optimization pointwise in time. For many control applications, a closed-loop Lyapunov function could be directly employed as a candidate CLF.*

C. Geometric Control Lyapunov Function

We consider the problem of tracking a desired reference state $(q_d, \dot{q}_d) \in TM$.

***Definition* 1.** *A smooth function $V : [0, \infty) \times TM \to \mathbb{R}$ is called a geometric ES-CLF for the system in* (3) *if there exist constants $c_1, c_2, \eta > 0$ such that*

$$\begin{aligned} &V(t, q, \dot{q}) \ge c_1(\Psi(q, q_d) + \langle\!\langle e_{\dot{q}}, e_{\dot{q}} \rangle\!\rangle), \\ &V(t, q, \dot{q}) \le c_2(\Psi(q, q_d) + \langle\!\langle e_{\dot{q}}, e_{\dot{q}} \rangle\!\rangle), \\ &\inf_{u \in \mathbb{R}^m} \{\frac{\partial V}{\partial t} + \underbrace{\langle d_1V, \dot{q}\rangle - \langle d_2V, M_q^{-1}dV_q\rangle}_{\text{equivalent to } L_fV} \\ &+ \underbrace{\textstyle\sum_{i=1}^m \langle d_2V, M_q^{-1}F_i\rangle}_{\text{equivalent to } L_{g_i}V} u_i + \eta V\} \le 0, \end{aligned} \tag{6}$$

holds for all $(t, q, \dot{q}) \in [0, \infty) \times TM$ where $e_{\dot{q}} = \dot{q} - \mathscr{T}_{(q,q_d)}\dot{q}_d$ and $u = [u_1, u_2, \cdots, u_m]^T$ is the vector containing all control inputs.

Note that the CLF $V(t, q, \dot{q})$ depends on the reference trajectory $q_d(t), \dot{q}_d(t)$ implicitly through the time t. Also, this generalized definition coincides with the previous one if the manifold is chosen to be $\mathbb{R}^{2n}$ and the reference point is chosen to be $(0, 0)$. The concept of geometric CLF is specifically useful for control design for systems whose configuration spaces are nonlinear manifolds, with dynamics given by (3).

D. Time-varying Control Barrier Function (CBF)

Control Barrier functions (CBFs) are defined with respect to a region in the state space. For the control affine system (5), suppose we have a continuously differentiable function $h : [0, \infty) \times \mathbb{R}^n \to \mathbb{R}$ with its super level set $\mathcal{C}_t = \{x \in \mathbb{R}^n : h(t, x) \geq 0\}$. If this set admits a non-empty interior at each time in $[0, \infty)$, then a smooth function $B : [0, \infty) \times \mathbb{R}^n \to \mathbb{R} \cup \{\pm\infty\}$ is called a CBF of $\mathcal{C}_t$ if there exist two class $\mathcal{K}$ function α_1, α_2 and $\mu > 0$ such that

$$\frac{1}{\alpha_1(h(x))} \leq B(t, x) \leq \frac{1}{\alpha_2(h(x))},$$
$$\inf_{u \in \mathbb{R}^m} \{\frac{\partial B}{\partial t} + L_f B + L_g B u - \frac{\mu}{B}\} \leq 0, \tag{7}$$

holds for any $t \in [0, \infty)$ and any $x \in \mathcal{C}_t^\circ$ which is the interior of $\mathcal{C}_t$.

***Remark* 3.** *The idea of a CBF is based on invariance analysis of a set for a dynamic system. To stay safe, the system trajectory should always remain within the safe set, $\mathcal{C}_t$, which entails that the safe set should be forward invariant for the closed loop system. By imposing condition* (7)*, we are able to set up a positive lower bound for the value of $h(t, x)$ that holds globally, which means that safety is guaranteed. Note that, the range of the CBF is chosen to be the extended real line which allows for the Barrier $B(t, x)$ to go to infinity as $h(t, x)$ goes to zero.*

E. Geometric Control Barrier Function

Similar to the case of CLF, we extend the concept of CBF to simple mechanical systems (3) evolving on manifolds. Because we can only analyze a set with respect to a specific topology, the topology on the configuration manifold M is considered to be the relative topology with respect to the smallest Cartesian space in which M can be embedded smoothly.

***Definition* 2.** *Suppose there exist a smooth function $h : [0, \infty) \times TM \to \mathbb{R}$ such that the safety region is defined by $\mathcal{C}_t = \{(q, \dot{q}) \in TM : h(t, q, \dot{q}) \geq 0\}$ which has nonempty interior for any $t \in [0, \infty)$. Then a smooth function $B : [0, \infty) \times \mathbb{R} \to \mathbb{R} \cup \{\pm\infty\}$ is called a geometric CBF of $\mathcal{C}_t$ if there exist two class $\mathcal{K}$ functions α_1, α_2 and a constant $\mu > 0$ such that*

$$\frac{1}{\alpha_1(h(t,q,\dot{q}))} \leq B(h(t, q, \dot{q})) \leq \frac{1}{\alpha_2(h(t,q,\dot{q}))},$$
$$\inf_{u \in \mathbb{R}^m} \{\frac{\partial B}{\partial t} + \underbrace{B'(h)\left(\langle d_1 h, \dot{q}\rangle - \langle d_2 h, M_q^{-1} dV_q\rangle\right)}_{\text{equivalent to } L_f B}$$
$$+ \underbrace{B'(h)\left(\textstyle\sum_{i=1}^m \langle d_2 h, M_q^{-1} F_i\rangle\right)}_{\text{equivalent to } L_{g_i} B} u_i - \frac{\mu}{B}\} \leq 0, \tag{8}$$

for any $t \in [0, \infty)$ and $x \in \mathcal{C}_t^\circ$.

***Remark* 4.** *Note that the time-varying CBF, as a scalar function, is purely based on the region function h. Both time and system state are implicitly contained within the CBF through the scalar function h. Thus, to design a CBF in this type, we just need to choose a suitable shape of this scalar function.*

The following Lemma provides a formal guarantee of safety.

***Lemma* 1.** *(Safety Guarantee of Time-varying Geometric CBF in* (8)*) For the system* (5)*, if the control input u satisfies the condition* (8) *at each time $t \in [0, \infty)$, then the set $\{x \in \mathbb{R}^n : h(t, x) > 0\}$ is forward invariant, i.e, the system trajectory $(q(t), \dot{q}(t))$ would always remain within $\mathcal{C}_t^\circ$ if $(q(0), \dot{q}(0)) \in \mathcal{C}_{t=0}^\circ$.*

Proof: See Appendix. A. ∎

Based on the concepts of geometric CLF and CBFs, we are able to propose a general method to construct CLF and CBF for system (3) in the next section. Table I summarizes the meanings of each symbol for further reference.

III. Safety Critical Control Design on Riemmanian Manifold

In this section, we will propose a general method to extend configuration constraints, given in terms of only the configuration variable q, to the whole state space $(q, \dot{q})$ so as to enforce the configuration constraints thereby maintaining safety. Following this, a candidate geometric CBF will be constructed and combined with a candidate geometric CLF. Based on the combination of the geometric CBF and CLF, we will propose a feedback controller through a state-dependent quadratic program that is solved point-wise in time.

A. Control Problem Formulation

Given a fully actuated simple mechanical system (3) and a list of time-varying safety constraints in terms of the configuration variables q, written as $g_i(t, q) \geq 0$ for $i \in \{1, 2, \cdots, k\}$, where

$$g_i(t, q) := (-1)^{\delta_i}(b_i(t) - \Psi(q, q_i(t))), \tag{9}$$

with $\delta_i \in \{0, 1\}$, $b_i(t) > 0$ representing the radius, $q_i(t) \in M$ representing the center and $\Psi(q, q_i(t))$ being the configuration error between the current configuration q. We can then define a time-varying safe set,

$$\mathcal{B}_{i,t} := \{(q, \dot{q}) \in TM : \ g_i(t, q) \geq 0, \quad q_i \in M\}, \tag{10}$$

satisfying the condition that

$$(\cap_{i=1}^k \mathcal{B}_{i,t})^\circ =: (\mathcal{B}_t)^\circ = \mathcal{B}_t^\circ \neq \varnothing \tag{11}$$

where the set $\mathcal{B}_{i,t}$ is the safety region for constraint g_i, and $\mathcal{B}_t^\circ$ denotes the interior of the set $\mathcal{B}_t$ with respect to the topology of the manifold M.

***Remark* 5.** *The constraints presented here are in terms of the configuration error. The value of δ_i is to indicate whether the inside or outside of the region $\mathcal{B}_{i,t}$ is safe or not. The center point $q_i : [0, \infty) \to M$ and the radius $b_i : [0, \infty) \to (0, \infty)$ are both sufficiently smooth. In real applications, these regions could be constructed through methods in computational geometry. By picking specific configuration errors, we are able to approximate the actual safe region in a proper way. For*

example, level sets of L_2, L_1, L_∞ norms on $\mathbb{R}^2$ could be a circle or squares with different orientations. We can choose a specific norm that could best fit the actual safe region through optimization.

The above compatible condition in (11) *is to ensure that the set of all specified constraints* can be satisfied at the same time. *The geometric intuition is that the corresponding free space is nonempty.*

With the above definitions, we are now in a position to state the control problem as follows.

Geometric constrained control problem: Given a smooth reference curve $q_d(t) \in \mathcal{B}_t^\circ$ for any $t \in [0, \infty)$, design the feedback control input $u = u(t, q, \dot{q})$ so that the following conditions are satisfied:

$$\begin{aligned} &q(t) \in \mathcal{B}_t, \ \forall t \in [0, \infty) && \text{(Safety Constraints)} \\ &q(t) \to q_d(t) \in \mathcal{B}_t \text{ as } t \to +\infty && \text{(Stability Constraints)} \end{aligned} \tag{12}$$

B. Geometric CBF Candidate

Having formulated the control problem, we now construct a geometric CBF to enforce safety. In particular, based on the configuration constraint functions g_i in (9), we propose a general method which can expand the safety region in configuration space M to the state space TM. We choose a smooth class $\mathcal{K}$ function $\beta : [0, \infty) \to \mathbb{R}$ and define a new constraint function in terms of t and $(q, \dot{q})$ as:

$$h_i(t, q, \dot{q}) = \gamma_i \beta(g_i(t, q)) + \langle d_1 g_i, \dot{q} \rangle + \frac{\partial g_i}{\partial t}. \tag{13}$$

Note that h_i is well-defined since dg_i is an one-form on M and thus it's a *linear functional* of the tangent space at each point q, and by the Chain rule, additional partial derivatives with respect to time can be expressed as:

$$\frac{\partial g_i}{\partial t} = (-1)^{\delta_i}(\dot{b}_i - \langle d_2 \Psi_{q,q_i}, \dot{q}_i \rangle).$$

Here, we have rewritten the configuration error $\Psi(q, q_i)$ as Ψ_{q,q_i} for symbolic simplicity.

We can then define a new expanded safety region in TM as:

$$\mathcal{C}_t := \cap_i^m \mathcal{C}_{i,t} := \cap_i^m \{(q, \dot{q}) \in TM : h_i(t, q, \dot{q}) \geq 0\} \tag{14}$$

where the parameters γ_i and $\beta(\cdot)$ are chosen to make sure the interior of $\mathcal{C}_t$ nonempty.

Question arises as whether the construction of $\mathcal{C}_t$ is meaningful or not. To be more precise, we expect the set $\mathcal{C}_t$ to be a nonempty set with some good properties for future analysis. We have listed the properties of $\mathcal{C}_t$ in the following lemmas.

***Lemma* 2.** *(Nonemptyness of $\mathcal{C}_t$ for the General Case)*

Suppose that the free space $\mathcal{B}_t$ is nonempty for each time $t \geq 0$. Also, there exist parameters $c_1, c_2, \cdots, c_k > 0$ such that $c_i g_i(t, q) \geq |\partial_t g_i(t, q)|$ for each $t \geq 0$ and each $q \in \mathcal{B}_t$, then there exist a Class $\mathcal{K}$ function $\beta(\cdot)$ and parameters $\gamma_1, \gamma_2, \cdots, \gamma_k > 0$ in Eq. (13) *which makes the corresponding $\mathcal{C}_t$ nonempty.*

Proof: See Appendix B. ■

Lemma. 2 provides a sufficient condition for the derivatives of $\dot{b}_i$ in order to make the set $\mathcal{C}_t$ nonempty. In particular, for the case when b_i is a constant, the condition of Lemma. 2 is automatically satisfied, and thus we have created a nonempty set $\mathcal{C}_t$ to work on. Moreover, from this lemma, we know that for each $q \in \mathcal{B}_t$, all the feasible tangent vectors $\dot{q}$ form a polyhedron in the linear space $T_q M$, which is based on the linear constraint in Eq. (31). The following lemma is about the relationship between the connectedness of $\mathcal{B}_t$ and $\mathcal{C}_t$. In particular, we will be focused on the time-invariant case for simplicity.

***Lemma* 3.** *(Connectedness of $\mathcal{C}_t$ for the Static Case)*

If the following conditions are satisfied:

- *There exist parameters γ_i and function $\beta(\cdot)$ such that $\mathcal{C}_t$ is nonempty.*
- *Both q_i and b_i are time-invariant.*
- *The set $\mathcal{B}_t$ has nonempty interior $\mathcal{B}_t^\circ$, and $\mathcal{B}_t^\circ$ is path connected.*

Then a subset $\mathcal{C}_t^B$ of $\mathcal{C}_t$, defined as $\{(q, \dot{q}) \in \mathcal{C}_t : q \in \mathcal{B}_t^\circ\}$ is also path connected.

Proof: See Appendix C. ■

The previous lemma establishes a relationship between the connectedness of the original constraint set $\mathcal{B}_t$ and part of the expanded set denoted as $\mathcal{C}_t^B$. In summary, the previous two lemmas justify the construction method of $\mathcal{C}_t$ in Eq. (13). The argument provided does not include the general time-varying case, but sheds some light on the construction of the set $\mathcal{C}_t$. The previous argument has set up some relationship between $\mathcal{B}_t$ and $\mathcal{C}_t$ only from the perspective of manifold. As already noticed in the proof, when $(q, \dot{q}) \in \mathcal{C}_t$, it's possible that $g(q)$ could be negative and consequently $q \notin \mathcal{B}_t$. Moreover, taking the dynamics into account, we could infer the safety properties of $\mathcal{B}_t$ and $\mathcal{C}_t$ in the lemma below.

***Proposition* 1.** *(Forward Invariance Preservation of the Feasible Region $\mathcal{B}_t$)*

Suppose the region $\mathcal{C}_t$ is forward invariant for the system (3)*, then the region $\mathcal{B}_t$ is also forward invariant whenever initially $q_0 \in \mathcal{B}_{t=0}$ and $(q_0, \dot{q}_0) \in \mathcal{C}_{t=0}$.*

Proof: See Appendix. D. ■

***Remark* 6.** *This proposition guarantees that if we could enforce the forward invariance of region $\mathcal{C}_t$, the safety constraints $(g_i(t, q, \dot{q}) \geq 0)$ are satisfied automatically. Equivalently, the previous constrained control problem* (12) *could be converted to a new problem below:*

$$\begin{aligned} &(q(t), \dot{q}(t)) \in \mathcal{C}_t, \ \forall t \in [0, \infty) \\ &(q(t), \dot{q}(t)) \to (q_d(t), \dot{q}(t)) \in \mathcal{C}_t \text{ as } t \to +\infty \end{aligned}$$

Based on the new region $\mathcal{C}_{i,t}$ in (14), we propose the following CBF candidate for each constraint in terms of h_i:

$$B_i(q, \dot{q}) = \frac{1}{h_i(t, q, \dot{q})}, \quad (q, \dot{q}) \in \mathcal{C}_t^\circ$$

Differentiating each B_i with respect to time yields,

$$\begin{aligned}\dot{B}_i(t,q,\dot{q}) = & -\frac{1}{h_i^2}\dot{h}_i(q,\dot{q}) \\ = & -\frac{1}{h^2}(\gamma_i\beta'(g_i)\langle d_1 g_i,\dot{q}\rangle + \langle \nabla_{\dot{q}} d_1 g_i,\dot{q}\rangle) \\ & + \frac{1}{h^2}\langle d_1 g_i, M_q^{-1} dV_q\rangle - \frac{1}{h^2}\sum_{i=1}^{m}\langle d_1 g_i, M_q^{-1}F_i\rangle u_i \\ & + \frac{(-1)^{\delta_i+1}}{h^2}(\ddot{b}_i - d_1 d_2\Psi_{q,q_i}(\dot{q},\dot{q}_i) \\ & - d_2 d_2\Psi_{q,q_i}(\dot{q}_i,\dot{q}_i) - \langle d_2\Psi_{q,q_i}, \nabla_{\dot{q}_i}\dot{q}_i\rangle).\end{aligned}$$

where M_q is the inertia metric, $d_1 d_2\Psi$ is the differential 2-form as introduced in (1), and the last term is the equivalent of second derivative of $\partial h/\partial t$ on the manifold.

In order to make sure each B_i is a CBF, the following condition should be satisfied:

$$\inf_{u\in\mathbb{R}^m}\{\dot{B}_i - \frac{\mu_i}{B_i}\} \le 0, \quad \forall (q,\dot{q}) \in \mathcal{C}_t,\ \forall j \in \{1,2,\cdots,k\}$$

which is equivalent to

$$\inf_{u\in\mathbb{R}^m}\{-\dot{h}_i - \mu_i h_i^3\} \le 0, \quad \forall (q,\dot{q}) \in \mathcal{C}_t,\ \forall j \in \{1,2,\cdots,k\} \quad (15)$$

where $\mu_i > 0$ is the increasing rate of the value of B_i as the state moves closer to the boundary.

This condition would fail when the m dimensional vector

$$[\langle dg_i, M_q^{-1}F_1\rangle, \langle dg_i, M_q^{-1}F_2\rangle, \cdots, \langle dg_i, M_q^{-1}F_m\rangle]^T$$

is a zero vector in Cartesian space because otherwise, we could always use a nonzero control input to cancel out all the other terms in 15. Using the fact that system (3) is *fully-actuated* and that the inertia metric M_q is *non-degenerate*, the condition is equivalent to that $dg_i = (-1)^{\delta_i+1} e_q(q,q_i) = 0$ in the cotangent space.

By the definition of the position error e_q, the set $\mathcal{D}_{i,t}^B = \{(q,\dot{q}) \in \mathcal{C}_t : e_q(q,q_i) = 0\}$ has *measure zero* in M for any $t \in [0,\infty)$. Then by sub-additivity of measure, it follows that

$$\mathcal{D}_t^B := \cup_{i=1}^m \mathcal{D}_{i,t}^B \Rightarrow \mu_L(\mathcal{D}_t^B) \le \sum_{i=1}^m \mu_L(\mathcal{D}_{i,t}^B) = 0, \quad (16)$$

where $\mu_L(\mathcal{T})$ is the Lebesgue measure of a measurable set $\mathcal{T}$.

Hence, the CBFs defined here hold everywhere except for a set with measure zero. So the candidate function proposed is an almost globally valid CBF.

Remark 7. *Although we haven't given a rigorous definition of Lebesgue measure on manifolds, it can be roughly treated as an estimation of the area of the manifold under study. Thus it is intuitive that any lower dimensional compact submanifold should have measure 0 since we could cover it using a strip with infinitesimal area. In fact, if we want to sample points uniformly from the configuration manifold, the probability of getting points on the lower dimensional compact submanifold is always zero. We refer to [25] for a more formal introduction.*

In order to present the feedback controller in a more concise manner, we denote the terms in $\dot{h}_i$ which multiply u as

$$\phi_0^i(t,q,\dot{q}) = [\langle dg_i, M_q^{-1}F_1\rangle, \cdots, \langle dg_i, M_q^{-1}F_m\rangle]^T,$$

and the terms in $\dot{h}_i$ which are independent of u as $\phi_1^i(t,q,\dot{q})$. In this way, the condition (15) which the CBF must satisfy could be reformulated as finding a control input u s.t.,

$$-(\phi_0^i \cdot u + \phi_1^i + \mu_i h_i^3) \le 0, \quad i \in \{1,2,\cdots,k\}. \quad (17)$$

C. Geometric CLF Candidate

From Section II, a candidate CLF has the expression as:

$$V(t,q,\dot{q}) = \alpha\Psi(q,q_d) + \frac{1}{2}\langle\!\langle e_{\dot{q}}, e_{\dot{q}}\rangle\!\rangle + \varepsilon\langle e_q, e_{\dot{q}}\rangle$$

where the coefficients $\alpha,\varepsilon > 0$ are chosen specifically to make V quadratic in terms of e_q and $e_{\dot{q}}$.

Differentiating it with respect to t gives us an expression which includes the control input explicitly as:

$$\begin{aligned}\dot{V} = & \alpha\langle d_1\Psi, e_{\dot{q}}\rangle - \langle\!\langle e_{\dot{q}}, [\frac{d}{dt}\Big|_{q \text{ fixed}}(\mathscr{T}\dot{q}_d) + (\nabla_{\dot{q}}\mathscr{T})\dot{q}_d]\rangle\!\rangle \\ & + \varepsilon[\langle\nabla_{e_{\dot{q}}}(e_q), e_{\dot{q}}\rangle - \langle d_1\Psi, ((\nabla_{e_{\dot{q}}}\mathscr{T})e_{\dot{q}})\rangle] \\ & - \varepsilon\langle e_q, [\frac{d}{dt}\Big|_{q \text{ fixed}}(\mathscr{T}\dot{q}_d) + (\nabla_{\dot{q}}\mathscr{T})\dot{q}_d]\rangle \\ & - [\varepsilon\langle d_1\Psi, M_q^{-1}dV_q\rangle + \langle\!\langle e_{\dot{q}}, M_q^{-1}dV_q\rangle\!\rangle] \\ & + \sum_{i=1}^m[\varepsilon\langle d_1\Psi, M_q^{-1}F_i u^i\rangle + \langle\!\langle e_{\dot{q}}, M_q^{-1}F_i u^i\rangle\!\rangle]\end{aligned}$$

Applying a similar argument to this CLF candidate, as we did for the geometric CBF, we have that only when the vector

$$\psi_0(t,q,\dot{q}) := \begin{bmatrix}[\varepsilon\langle e_q, M_q^{-1}F_1\rangle + \langle\!\langle e_{\dot{q}}, M_q^{-1}F_1\rangle\!\rangle] \\ [\varepsilon\langle e_q, M_q^{-1}F_2\rangle + \langle\!\langle e_{\dot{q}}, M_q^{-1}F_2\rangle\!\rangle] \\ \vdots \\ [\varepsilon\langle e_q, M_q^{-1}F_n\rangle + \langle\!\langle e_{\dot{q}}, M_q^{-1}F_m\rangle\!\rangle]\end{bmatrix}$$

becomes zero, the CLF condition (6) fails to hold. By the definition of the position and velocity errors, $e_q, e_{\dot{q}}$, the region

$$\mathcal{D}_t^V = \{(q,\dot{q}) \in \mathcal{C}_t : \psi_0(q,\dot{q}) = 0\} \quad (18)$$

has measure zero for any $t \in [0,\infty)$. Hence almost global property also holds for this type of CLF. By denoting the net term which doesn't depend on u as $\psi_1(t,q,\dot{q})$, the condition imposed by this CLF could be written as:

$$\psi_0 \cdot u + \psi_1 + \eta V \le 0 \quad (19)$$

where $\eta > 0$ indicates the convergent rate of CLF.

So far we know the condition of CLF and CBF would only fail to be satisfied for the set $\mathcal{D}_t = \mathcal{D}_t^B \cup \mathcal{D}_t^V$, with $\mathcal{D}_t^B, \mathcal{D}_t^V$ as defined in (16), (18), where at least one of the vectors ϕ_0^i in (17), ψ_0 in (19) become zero. We call it *singularity set* of Ψ which depends on the specific configuration error chosen. Note that the singularity here isn't referring to that of the local coordinate, but rather it is related to the specific properties of CBF and CLF.

D. CBF-CLF-QP Control Design for Fully Actuated, Simple Mechanical Systems

The previous subsections have introduced geometric CBFs and CLFs for the general mechanical systems which hold almost globally. Now we are able to combine them together in the control design using optimization.

First, decompose the total control input into two parts, the feed-forward and feedback components:

$$u = u_{ff} + u_{fb}$$

where the feed-forward term is directly computed as the solution of the linear equation below

$$\sum u^i_{ff} F_i = dV_q(q) + M_q[\frac{d}{dt}\Big|_{q \text{ fixed}} (\mathscr{T}\dot{q}_d) + (\nabla_{\dot{q}}\mathscr{T})\dot{q}_d]$$

which comes from [6] in geometric control.

Then compute the feedback term u^i_{fb} based on the following state-dependent optimization problem.

(CBF-CLF-QP Control Design):

Formulate the feedback control problem based on a state dependent Quadratic Programming (QP):

$$\begin{aligned}[u_{fb}, \delta^*] = \underset{v\in\mathbb{R}^m, \delta\in\mathbb{R}}{\operatorname{argmin}} \ & \frac{1}{2} v^T H v + \frac{1}{2}\lambda\delta^2 \\ \text{s.t.} \quad & \psi_0 \cdot v + [\psi_0 \cdot u_{ff} + \psi_1 + \eta V] \leq \ \delta, \\ & -(\phi^i_0 \cdot v + \phi^i_0 \cdot u_{ff} + \phi^i_1 + \mu_i h^3_i) \leq \ 0,\end{aligned} \tag{20}$$

where the weight matrix $H \in \mathbb{R}^{m\times m}$ is positive definite, and $\lambda > 0$ is the penalty weight for the relaxation parameter δ.

***Remark* 8.** *As discussed in [3], the constraints imposed by CBFs are treated as Hard Constraints that must be satisfied during the whole control process, while the constraint imposed by the CLF is a Soft Constraint with the relaxation parameter δ. The hard constraints are the safety-critical constraints. Also recall that $\alpha, \varepsilon, \eta > 0$ are scalars that are relevant to the CLF V while $\beta : \mathbb{R} \to \mathbb{R}, \gamma_i, \mu_i > 0$ are function and parameters that are relevant to each CBF B_i. These parameters can be tuned to improve the controller's performance in numerical implementations.*

***Remark* 9.** *In order to guarantee the existence and uniqueness of system trajectory, we require the control input should be at least piecewise continuous. We refer to [39], [26] for detailed discussion on the continuity of the solution of state dependent QPs. The solution is guaranteed to be Lipschitz continuous under certain conditions, which can be satisfied for our problem.*

The proposition below shows the safety guarantee of CBF-CLF-QP controller.

***Proposition* 2.** *(Safety Property of CBF-CLF-QP Controller) If the following conditions are satisfied:*

- *There exist proper parameters for both V and B_i, $i \in \{1, 2, \cdots, k\}$ such that the initial condition $(q_0, \dot{q}_0)$ stays within the expanded safety region $\mathcal{C}^\circ_t$.*
- *The singularity set $\mathcal{D}_t$ where CBF or CLF fail has measure zero.*
- *The online QP* (20) *has feasible solution for the set $\mathcal{C}_t \backslash \mathcal{D}_t$.*

then the trajectory of the closed loop system (3) *is safe for all $t \in [0, \infty)$.*

Proof: See Appendix E. ■

Having presented the general safety-critical control design using geometric CBFs and geometric CLFs, we next specialize the controller to some simple mechanical systems and present numerical results.

IV. Safety Critical Control for a 3D Point Mass

We begin by specializing the general construction presented in the previous section to a 3D-moving point mass in $\mathbb{R}^3$ by developing the associated geometric CLF and CBF, and presenting numerical results for both time-invariant and time-varying safety-critical constraints. In subsequent sections, this formulation is extended to a spherical pendulum in S^2 and a 3D pendulum in $SO(3)$.

Consider a single 3D point mass, with configuration space $\mathcal{Q} = \mathbb{R}^3$ with Cartesian position $q = [x, y, z]^T \in \mathcal{Q}$, velocity $\dot{q} \in T_q\mathcal{Q} = \mathbb{R}^3$, input $u = [u_1, u_2, u_3]^T \in \mathbb{R}^3$, and mass m, such that the system dynamics is $\ddot{q} = m^{-1}u$ with Riemannian metric $\langle\!\langle \dot{q}_1, \dot{q}_2 \rangle\!\rangle = m\dot{q}_1 \cdot \dot{q}_2$. Given a smooth reference trajectory $q_d \in \mathbb{R}^3$, the configuration error can be written as,

$$\Psi(q, q_d) = \|q - q_d\|^2 = (q - q_d) \cdot (q - q_d),$$

which is equipped with the differential,

$$e_q = d_1\Psi(q, q_d) = q - q_d, \quad d_2\Psi(q, q_d) = -(q - q_d).$$

The compatible transport map satisfying (2) is given by,

$$\mathscr{T}_{(q,q_d)}\dot{q}_d = \dot{q}_d \implies e_{\dot{q}} = \dot{q} - \dot{q}_d,$$

since we can directly compare two tangent vectors in $\mathbb{R}^3$.

Next, consider a list of safety constraints $g_i(q) = (-1)^{\delta_i}(b_i - \Psi(q, q_i)) \geq 0$ with $i \in \{1, 2, \cdots, k\}, b_i > 0$, wherein with our chosen configuration error Ψ, each constraint $g_i(q)$ represents the safe set as either a sphere centered at q_i or its complement, depending on the choice of $\delta_i \in \{0, 1\}$ respectively. The corresponding CLF and CBF candidates can be respectively constructed as:

$$\begin{aligned} V = & \frac{1}{2} m(\dot{q} - \dot{q}_d) \cdot (\dot{q} - \dot{q}_d) + \frac{\alpha}{2}(\|q - q_d\|^2) \\ & + \varepsilon(q - q_d) \cdot (\dot{q} - \dot{q}_d), \\ h_i = & \gamma_i g_i + (-1)^{\delta_i}[\dot{b}_i - 2(q - q_i) \cdot (\dot{q} - \dot{q}_i)], \\ B_i = & 1/h_i, \end{aligned} \tag{21}$$

where $\alpha > 0$ and $\gamma_i > 0$. Note that the feedforward input is given by $u_{ff} = m\ddot{q}_d$. We incorporate the above into the online QP in (20). Also, using the definitions in (16) and (18), we can specify the singular sets as

$$\begin{aligned} \mathcal{D}^V_t = & \{(q, \dot{q}) \in \mathbb{R}^6 : me_{\dot{q}} + \varepsilon e_q = 0\}, \\ \mathcal{D}^B_t = & \cup^k_{i=1} \{(q, \dot{q}) \in \mathbb{R}^6 : q = q_i\}, \end{aligned}$$

which are the union of several curves in $T\mathcal{Q} \simeq \mathbb{R}^6$ and thus have measure zero.

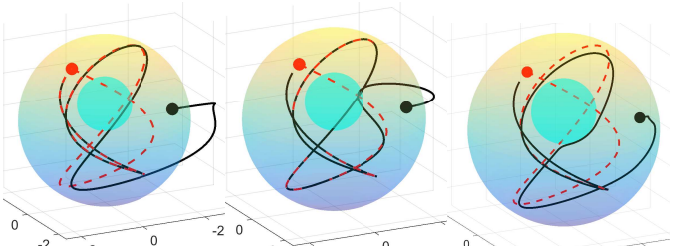

(a) Min-Norm (b) Geometric Control (c) CBF-CLF-QP

Fig. 1: *(3D Point Mass with Time-Invariant Safety Constraints)*: Simulation of various controllers on the point mass system on $\mathbb{R}^3$, which is required to track a desired trajectory while being restricted to move within the region between two spheres. As can be seen for (a) min-norm, and (b) geometric control, the system trajectory exits the outer sphere as well as enters the inner sphere, violating critical safety region constraints. However, for (c) CLF-CBF-QP controller, the critical safety constraint is enforced while still following the desired trajectory.

A. 3D Point Mass with Time-Invariant Safety Constraints

Based on the previous discussion, we present numerical validation our proposed controller. We consider a point mass with $m = 2.5kg$ moving strictly inside a large safety region ($g_1(q) \geq 0$) and avoiding a small spherical obstacle inside the safety region ($g_2(q) \geq 0$) while tracking a desired reference trajectory $q_d(t)$, which in the extreme case, passes directly through the obstacle (see red dashed line in Fig. 1). These safety constraints are

$$\begin{aligned} g_1 &= (-1)^0(2.5^2 - \Psi(q,[0,0,0]^T)) \geq 0, \\ g_2 &= (-1)^1(0.85^2 - \Psi(q,[0,0,0.5]^T)) \geq 0, \end{aligned} \tag{22}$$

while the reference trajectory is $q_d(t) = [-0.5\sin 1.5t, 1.25\cos(1.25t+\pi/4), 0.75\cos(0.75t+\pi/6)]^T$.

We compare the performance of three different controllers, a geometric CLF min-norm controller, traditional geometric controller from [6], and our proposed geometric CBF-CLF-QP controller. The results in Fig. 1 show that the CBF-CLF-QP controller keeps the point mass away from boundary of the unsafe regions to strictly enforce the safety constraints encoded by the non-negativity of g_1, g_2 as seen in Fig. 2. We also plot the geometric CLF in Fig. 2 while highlighting the durations when the reference becomes unsafe. It can be seen that the actual trajectory exponentially tracks the reference when the reference is safe.

B. 3D Point Mass with Time-Varying Safety Constraints

We next consider time-varying safety constraints by introducing time-varying obstacles that the point-mass needs to avoid. In particular, we consider a desired reference trajectory $q_d(t) = [-\sin 1.25t, \cos 1.25t, 0]^T$, which is a circle in the XY plane centered at the origin. We require the point mass to stay within a safety region given by a ball of radius $r_0(t) \equiv 3.0$ centered at the origin (large transparent outer sphere in Fig.3) while avoiding the two sphere-shaped obstacles of radii

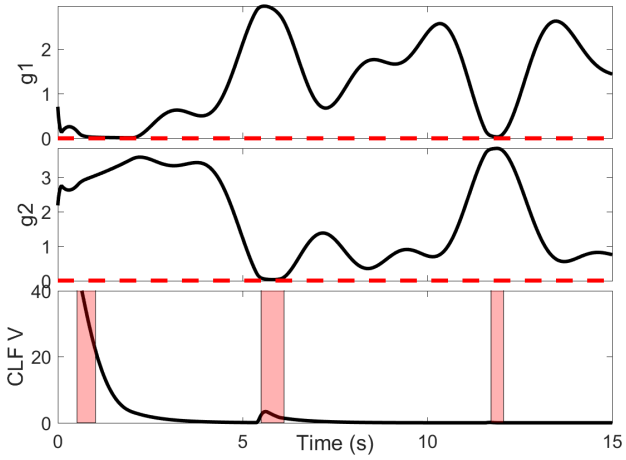

Fig. 2: *(3D Point Mass with Time-Invariant Safety Constraints)*: Plots of the constraint functions g_i and the geometric CLF V. The proposed controller ensures $g_i \geq 0$. Durations when the reference trajectory is unsafe are highlighted in red, during which the CLF could increase due to the relaxation δ in (20).

$r_1(t) = r_2(t) \equiv 0.15$ (two small spheres in Fig.3) that move along the circular reference trajectory in opposite directions with angular velocities $\omega_1 = 0.5$, $\omega_2 = 0.8$. To be precise, the corresponding safety constraints are given below as:

$$\begin{aligned} g_1 &= (-1)^0(r_0^2 - \Psi(q,0)) \geq 0, \\ g_2 &= (-1)^1(r_1^2 - \Psi(q,q_1(t))) \geq 0, \\ g_3 &= (-1)^1(r_2^2 - \Psi(q,q_2(t))) \geq 0, \end{aligned} \tag{23}$$

where $q_1(t) = [\cos(\omega_1 t), \sin(\omega_1 t), 0]^T, q_2(t) = [\sin(\omega_2 t), \cos(\omega_2 t), 0]^T$.

Fig.3 illustrates snapshots in time, wherein the motion of the obstacles are depicted through shaded regions and time is conveyed through change in transparency from light to dark. As can be seen, the actual trajectory (black solid) avoids the moving obstacles while trying to follow the desired trajectory (red dashed). The values of each constraint function g_i and the geometric CLF are plotted in Fig. 4. As can be seen, the controller ensures the non-negativity of the constraints. The periodic fluctuation is due to the reference trajectory encountering a moving obstacle every three seconds. When the reference trajectory becomes unsafe (indicated by red shared region), the controller relaxes tracking while ensuring safety.

***Remark* 10.** *As can be seen from Fig. 4, the value of the CLF could potentially increase in the red shaded regions, where the reference is unsafe. This is natural, since to remain safe we have to keep the system state away from the unsafe reference. Typically this is realized either through re-planning of the desired reference or through switched control schemes which are turned on when the actual state is close to the unsafe region. In contrast, due to the existence of the relaxation*

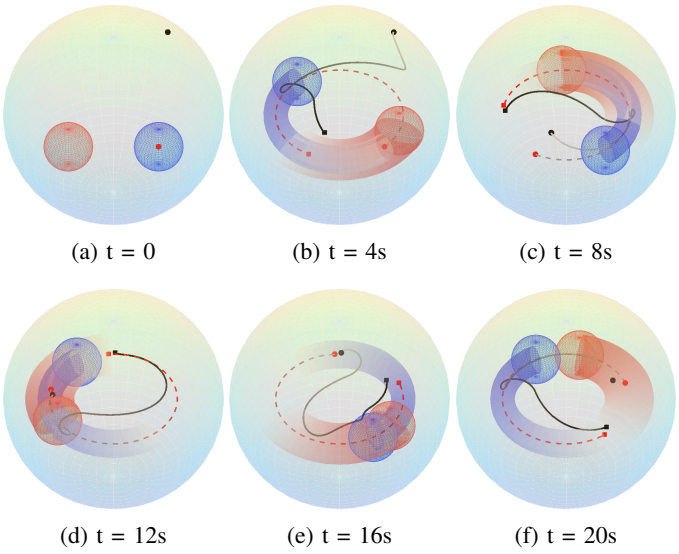

(a) t = 0 (b) t = 4s (c) t = 8s

(d) t = 12s (e) t = 16s (f) t = 20s

Fig. 3: *(3D Point Mass with Time-Varying Safety Constraints)*: Snapshots of a 3D moving point mass subject to following a desired trajectory while avoiding dynamic obstacles are shown. Each snapshot illustrates the past four seconds of the actual trajectory of the point-mass (black solid) and the desired trajectory (red dashed), with start and end positions marked by small circle and square markers respectively. Increasing time is conveyed by a change in transparency from light to dark. An animation video is available at https://youtu.be/IwY7fvF1SFk.

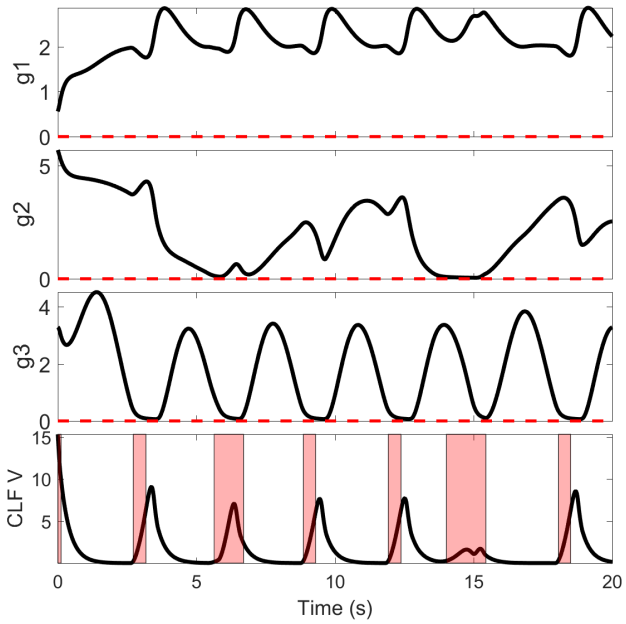

Fig. 4: *(3D Point Mass with Time-Varying Safety Constraints)*: Plots of constraint functions g_i and the geometric CLF V. The proposed controller ensures $g_i \geq 0$. Durations when the reference trajectory is unsafe are highlighted in red.

parameter δ in the online QP (20)*, we are able smoothly mediate between stable tracking of the reference and staying safe when the reference is unsafe.*

V. Safety Critical Control for a Spherical Pendulum

We next consider a spherical pendulum system that comprises of a point mass connected to a pivot through a massless rod as shown in Fig. 5. The configuration of this system is given by the unit sphere $\mathbb{S}^2$. Using the directional vector $q \in \mathbb{S}^2$ corresponding to the unit vector from the pendulum pivot to the point mass, we have the dynamical equation given as,

$$\begin{aligned} \dot{q} &= \omega \times q, \\ \dot{\omega} &= q \times (\tfrac{F}{ml} - \tfrac{g}{l} e_3), \end{aligned} \qquad \text{or} \quad \ddot{q} + (\dot{q}\cdot\dot{q})q = -\hat{q}^2(\frac{F}{ml} - \frac{g}{l}e_3),$$

which is a fully-actuated simple mechanical system since the tangential force could span the tangent space at each point on the sphere.

Denote a normalized force $u := (F/ml - g/l e_3)$ and thus the system dynamics could be simplified as:

$$\ddot{q} + (\dot{q}\cdot\dot{q})q = -\hat{q}^2 u, \tag{24}$$

where there are no mass parameters. Here the hat map $\hat{\cdot} : \mathbb{R}^3 \to \mathfrak{so}(3)$ converts a three-dimensional vector to a skew-symmetric real matrix. For this system, the Riemmanian metric

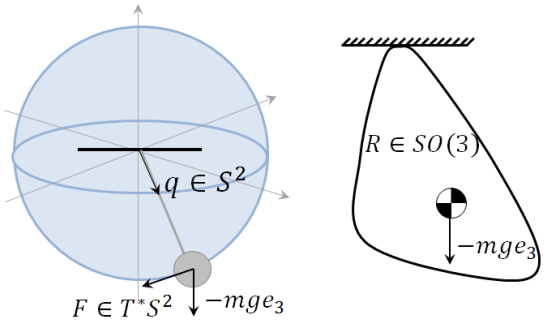

Fig. 5: Diagram of the spherical and 3D pendulums.

degenerates to the normal inner product $\langle\!\langle \dot{q}_1, \dot{q}_2 \rangle\!\rangle = \dot{q}_1 \cdot \dot{q}_2$. The configuration error can be defined as:

$$\Psi(q, q_d) = 1 - q \cdot q_d, \quad e_q = d_1\Psi = \hat{q}^2 q_d, \quad d_2\Psi = \hat{q}_d^2 q.$$

The compatible transport map and velocity error are given by:

$$\mathscr{T}_{(q,q_d)}\dot{q}_d = (q_d \times \dot{q}_d) \times q \implies e_{\dot{q}} = \dot{q} - (q_d \times \dot{q}_d) \times q.$$

Next, given a smooth reference trajectory $q_d \in \mathbb{S}^2$ and a list of constraints $g_i = (-1)^{\delta_i}(b_i - \Psi(q, q_i)) \geq 0$ where $b_i \in (-1, 1)$,

the corresponding CLF and CBF are given as

$$V = \frac{1}{2} e_{\dot{q}} \cdot e_{\dot{q}} + \frac{1}{2}\alpha(1 - q \cdot q_d) + \varepsilon e_q \cdot e_{\dot{q}}, \tag{25}$$
$$h_i = \gamma_i g_i + (-1)^{\delta_i}(q_i \cdot \dot{q} + \dot{q}_i \cdot \dot{q} - \dot{b}_i),$$
$$B_i = 1/h_i,$$

where $\delta_i \in \{0, 1\}$, and $\gamma_i > 0$.

The constraint defined here could be visualized as a cone centered at q_i bounded by the radius b_i. Depending on the value of δ_i, the cone is treated as either unsafe or safe region. The corresponding feedforward input is $u_{ff} = (q_d \times \ddot{q}_d) \times q - \hat{q}^2(q_d \times \dot{q}_d) \times \dot{q}$, which is used by the controller (20).

In order to analyze the singularity set $\mathcal{D}_t$, we write out the vectors in (16) and (18) explicitly as

$$\phi_0^i = (-1)^{\delta_i} q_i, \quad \psi_0^i = (e_{\dot{q}} + \varepsilon e_q).$$

The corresponding singularity set for the spherical pendulum could be defined as:

$$\mathcal{D}_t^V = \{(q, \dot{q}) \in T\mathbb{S}^2 : e_{\dot{q}} + \varepsilon e_q = 0\},$$
$$\mathcal{D}_t^B = \cup_{i=1}^{k} \{(q, \dot{q}) \in T\mathbb{S}^2 : q = \pm q_i\},$$

which also has measure zero in the state space.

A. Spherical Pendulum with Time-Invariant Safety Constraints

Using the above formulations for the spherical pendulum, we compare the performance of the geometric min-norm, geometric controller in [6], and the proposed geometric CBF-CLF-QP controller for the normalized system (24). In this scenario, the safety region is defined to be the difference of two cone regions on the unit sphere $\mathbb{S}^2$. The corresponding safety constraints are given as:

$$g_1 = (-1)^0(\cos(\pi/12) + 1 - \Psi(q, q_n)) \geq 0,$$
$$g_2 = (-1)^1(\cos(\pi/4) + 1 - \Psi(q, q_n)) \geq 0, \tag{26}$$

which represent the outer and inner cones respectively in Fig. 6, with the static center point given by $q_n = [0, 0, -1]^T$.

The results in Fig. 6 illustrate that our proposed controller is able to keep the pendulum outside the inner (red) unsafe cone and inside the outer (blue) safe cone, thereby guaranteeing the safety constraints encoded by the non-negativity of g_1, g_2 as seen in Fig. 7. The tracking convergence is illustrated by the CLF plot in Fig. 7.

B. Spherical Pendulum with Time-Varying Safety Constraints

We next consider time-varying safety constraints on $\mathbb{S}^2$ by introducing two time-varying cone constraints, where the cone axis is specified through time-varying trigonometric functions with the cone radii held constant. In particular, the safety constraints are given as:

$$g_1 = (-1)^0(\cos(\pi/12) + 1 - \Psi(q, q_n(t))) \geq 0,$$
$$g_2 = (-1)^1(\cos(\pi/4) + 1 - \Psi(q, q_n(t))) \geq 0, \tag{27}$$

which represent the outer cone and inner cone separately, with the time-varying axis given by $q_n(t) = [\sin(\pi/5)\cos(0.25t), \sin(\pi/5)\sin(0.25t), -\cos(\pi/5)]^T$.

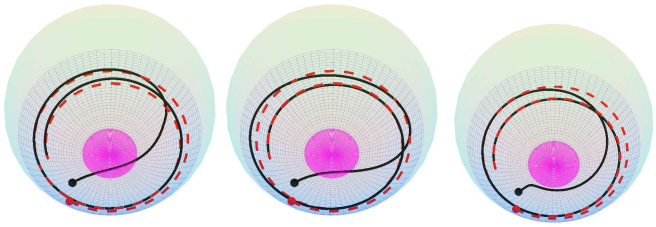

(a) Min-Norm (b) Geometric Control (c) CBF-CLF-QP

Fig. 6: *(Spherical Pendulum with Time-Invariant Safety Constraints)*: Simulation of various controllers on the spherical pendulum system on $\mathbb{S}^2$, restricted to remain between two cones in a unit sphere. The inner (magenta) cone represents the unsafe region while the outer (blue) cone represents the safe region. For (a) min-norm, and (b) geometric control, the system trajectory enters the unsafe inner cone area, whereas for (c) CBF-CLF-QP, the controller ensures the trajectory remains within the safe set while converging to the desired trajectory.

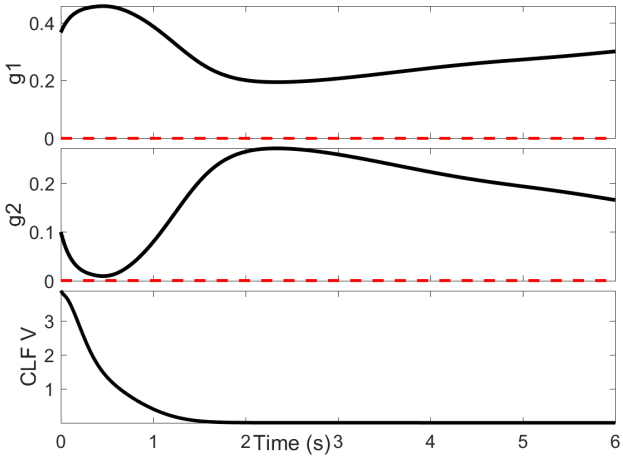

Fig. 7: *(Spherical Pendulum with Time-Invariant Safety Constraints)*: Plots of constraint functions g_i and the geometric CLF V. The proposed controller ensures $g_i \geq 0$.

Fig. 8 illustrates snapshots in time, where in the motion of the cones are depicted through shaded regions and time is conveyed through change in transparency from light to dark. The outer (blue) cone is safe, while the inner (red) cone is unsafe. The reference trajectory for the spherical pendulum is shown in red dashed line while the actual trajectory is drawn in black solid line. As seen in Fig. 9, the controller enforces the safety constraints while tracking the desired trajectory by maintaining the non-negativity of g_1, g_2. Fig. 9 also shows the plot of geometric CLF for the spherical pendulum. As can be seen, the value of CLF keeps decreasing when the reference is in the safe region and potentially increases when the reference

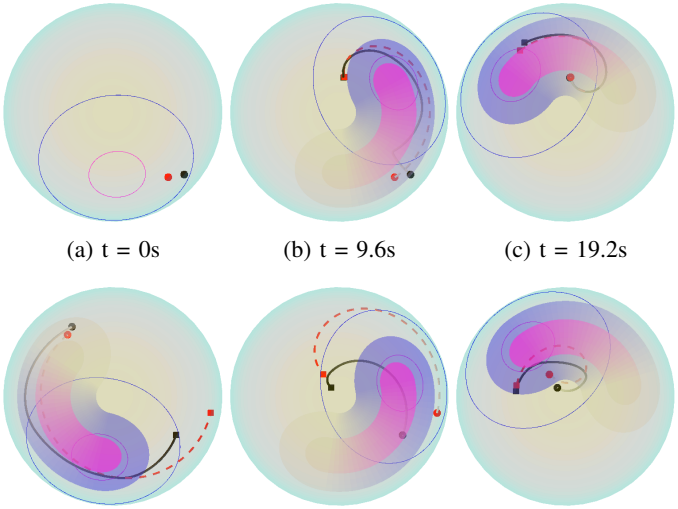

(a) t = 0s (b) t = 9.6s (c) t = 19.2s

(d) t = 28.8s (e) t = 38.4s (f) t = 48s

Fig. 8: *(Spherical Pendulum with Time-Varying Safety Constraints)*: Snapshots of a single spherical pendulum subject to two time-varying cone constraints are shown. The inner (red) cone is an obstacle which should be avoided while the outer (blue) cone is the safe region that the pendulum should remain within. The black solid line is the actual trajectory of the pendulum's point mass and the red dashed line represents the reference trajectory. The first snapshot shows the initial position and shape of the safety set. The rest of the snapshots show the inner and outer cones with changing transparency to indicate the progress of time. Each snapshot also shows the boundary of the cones at the ending time. An animation video is available at https://youtu.be/IwY7fvF1SFk.

is unsafe (highlighted by red region).

VI. Safety Critical Control for a 3D Pendulum

Having studied the evaluation of our controller on $\mathbb{R}^3, \mathbb{S}^2$, we next consider a 3D pendulum, as shown in Fig. 5, that evolves on $SO(3)$. The 3D pendulum comprises of a rigid body suspended at a pivot, with the orientation of the rigid body controlled by a torque exerted at the pivot. To be consistent with symbolic annotation in prior work, we use R and Ω to represent the orientation and angular velocity of the 3D pendulum, instead of $q, \dot{q}$ as used for the spherical pendulum. The system dynamics is given in [18] as:

$$\dot{R} = R\hat{\Omega}, \qquad J\dot{\Omega} = J\Omega \times \Omega + \tau,$$

where τ represents the torque at the pivot.

The configuration space $SO(3)$ is a Lie group and is a *smooth Riemannian manifold*. As a group, the manifold allows for multiplication and the existence of an identity. The tangent space at identity is called Lie algebra which can be identified with the tangent space at any point through left and right multiplication. More information about the properties of a Lie group can be found in [7]. The metric between two elements

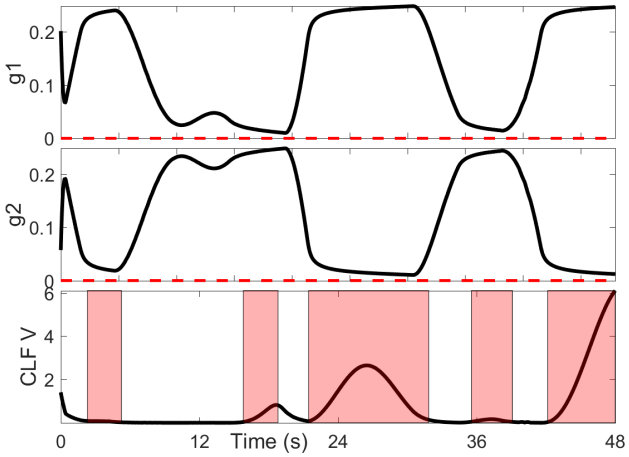

Fig. 9: *(Spherical Pendulum with Time-Varying Safety Constraints)*: Plots of constraint functions g_i and geometric CLF V. The proposed controller ensures $g_i \geq 0$.

$R, R_d \in SO(3)$ here is given by the *right attitude error* as:

$$\Psi(R, R_d) = \frac{1}{2}\mathrm{Tr}(I - R_d^T R).$$

To represent the tangent vector at R, we use the *body-fixed angular velocity* Ω that's related to $\dot{R}$ through the equation $\dot{R} = R\hat{\Omega}$. In this representation of body angular velocity, the corresponding position error could be given by:

$$e_R = d_1\Psi(R, R_d) = \frac{1}{2}(R_d^T R - R^T R_d)^\vee, \; d_2\Psi(R, R_d) = -e_R.$$

Note that the vector e_R is an element of the cotangent space. A compatible transport map is given by $\mathscr{T}_{(R,R_d)}(\Omega_d) = R^T R_d \Omega_d$ where $\Omega_d = (R_d^T \dot{R}_d)^\vee$, which is the desired angular velocity. Thus the velocity error has the expression $e_\Omega = \Omega - R^T R_d \Omega_d$.

Then, given a smooth reference trajectory $R_d(t) \in SO(3)$ and a list of constraints $g_i = (-1)^{\delta_i}(b_i - \mathrm{Tr}(I - R_i^T R)/2) \geq 0$, the corresponding geometric CLF and CBF candidates are:

$$\begin{aligned} V &= \frac{1}{2}e_\Omega^T J e_\Omega + \frac{1}{2}\alpha \cdot \mathrm{Tr}(I - R_d^T R) + \varepsilon e_R \cdot e_\Omega, \qquad (28)\\ h_i &= \gamma_i g_i + (-1)^{\delta_i}[\frac{1}{2}v_i \cdot (\Omega - \Omega_i) + \dot{b}_i],\\ B_i &= 1/h_i, \end{aligned}$$

where

$$v_i = \begin{bmatrix} (R_i^T R)_{23} - (R_i^T R)_{32} \\ (R_i^T R)_{31} - (R_i^T R)_{13} \\ (R_i^T R)_{12} - (R_i^T R)_{21} \end{bmatrix}, \; \Omega_i = (R_i^T \dot{R}_i)^\vee, \; b_i \in (0, 2),$$

and the feedforward term is given as:

$$\tau_{ff} = \Omega \times J\Omega + J(-\hat{\Omega}R^T R_d \Omega_d + R^T R_d \dot{\Omega}_d).$$

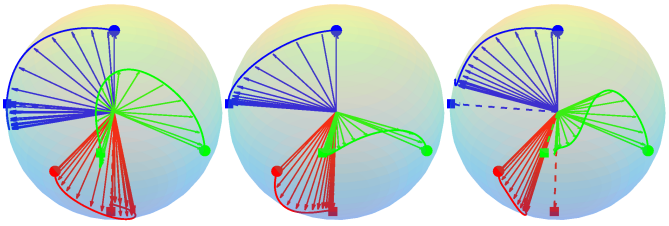

(a) Min-Norm (b) Geometric Control (c) CBF-CLF-QP

Fig. 10: *(3D Pendulum with Time-Invariant Safety Constraints)*: Comparison between various controllers for the 3D pendulum on $SO(3)$. The trajectories of all three directional vectors are plotted out on a sphere for better visualization. Here we use the dashed line to illustrate the static reference R_d and set up a safe region as $\Psi(R, I) \leq 0.75$. As can be seen for (a) min-norm, and (b) geometric control, the actual rotation matrix would tend to desired one. However, for (c) CBF-CLF-QP controller, the actual rotation is forced a distance away from it due to the imposed safety constraint.

Following a similar derivation as in $\mathbb{S}^2$, we have the singularity set $\mathcal{D}_t$ on $SO(3)$ as below:

$$\mathcal{D}_t^V = \{(R, \Omega) \in TSO(3) : Je_\Omega + \varepsilon e_R = 0\},$$
$$\mathcal{D}_t^B = \cup_{i=1}^k \{(R, \Omega) \in TSO(3) : v_i = 0\},$$

which is also the union of several curves in the state space $TSO(3)$ and thus has measure 0.

A. 3D Pendulum with Time-Invariant Safety Constraints

We next consider numerical validation of our proposed controller on the 3D pendulum system. We consider a 3D pendulum, with inertia matrix $J = diag(0.1, 0.2, 0.5)$, and require it to track a goal orientation $R_d(t) \equiv \exp(\hat{\xi})$, where $\xi = [0.5, 1.5, 0]^T$, while enforcing a safety constraint given by

$$g = (-1)^0 \left(0.75 - \frac{1}{2}\text{Tr}(I - R)\right) \geq 0. \tag{29}$$

As before, we compare the performance of the min-norm, geometric, and geometric CBF-CLF-QP controllers. Fig. 10 illustrates the results of the comparison, wherein we depict the trajectories of each unit vector of the 3-axis rotation frame on a unit sphere $\mathbb{S}^2$. The circles on the sphere indicate the initial positions of each axis of the actual trajectory $R(t)$ while the squares represent the goal positions of each axis of the reference R_d. From the plot of the constraint function g in Fig. 11, we see that both the CLF-minnorm controller and the geometric controller violate the safety constraint (29), while the proposed CBF-CLF-QP controller on a Lie group ensures safety as seen by g being positive. Fig. 11 also illustrates the geometric CLF V. Since the goal is always in the unsafe region, the entire V plot is highlighted in red. Consequently, the controller decreases V to a nonzero constant, which indicates that the actual trajectory reaches a point which is the minimum of CLF in the safe region.

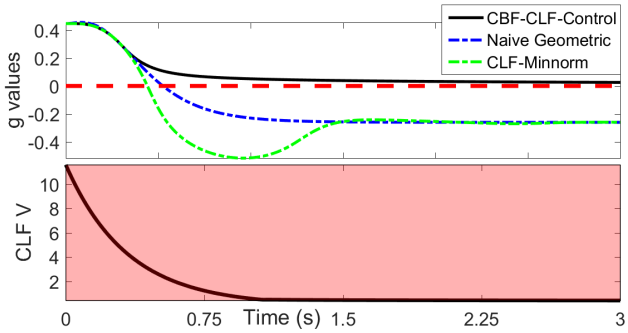

Fig. 11: *(3D Pendulum with Time-Invariant Safety Constraints)*: Plots of the constraint function g and the geometric CLF V. The values of g for both CLF-minnorm and geometric controllers are also plotted to illustrate the violation of safety for these controllers, while the proposed controller ensures $g \geq 0$.

B. 3D Pendulum with Time-Varying Safety Constraints

For $SO(3)$, considering time-varying constraints is of particular importance due to various applications in aerospace engineering. For instance, spacecraft have to constantly have sensitive instruments such as telescopes and radio antennae pointed around a particular axial frame towards a reference sensing object, while also making sure they are not pointed along another axial frame, at bright stars. These constraints can naturally be encoded through our CBFs on $TSO(3)$. Moreover, since the spacecraft and reference objects are relatively moving, this results in a time-varying safety constraint.

In this scenario, we test our CBF-CLF-QP controller's performance on attitude reorientation of a spacecraft subject to a single time-varying safety constraint that is specified by,

$$g = (-1)^1 \left(b(t) - \Psi(R, R_n(t))\right) \geq 0, \tag{30}$$

where $R_n(t) = \exp(\hat{\omega} t)$, $\omega = [1/2, 0, \sqrt{3}/2]^T$ and $b(t) = 0.8 + 0.4 \cos 2t$. Note that the safety constraint is constructed around a point rotating at a constant body-fixed angular velocity with a periodically changing size. The reference trajectory is given by:

$$R_d(t) \equiv \begin{bmatrix} 0 & 0 & 1 \\ 0 & 1 & 0 \\ -1 & 0 & 0 \end{bmatrix}.$$

which is selected so as to switch between being in the safe and unsafe regions.

Fig. 12 illustrates simulation results of our proposed controller. Fig. 12(a) shows the configuration error between the current orientation R and the center R_n and plots this along with b. From (30), to remain safe, the configuration error Ψ can never be larger than b at any time. As can be seen from the plot, the controller never violates safety. The corresponding value of g and the geometric CLF V are shown in Fig. 12(b), where the unsafe regions are highlighted in red. This shows that our CBF-CLF-QP controller can track the reference in a safety-critical way.

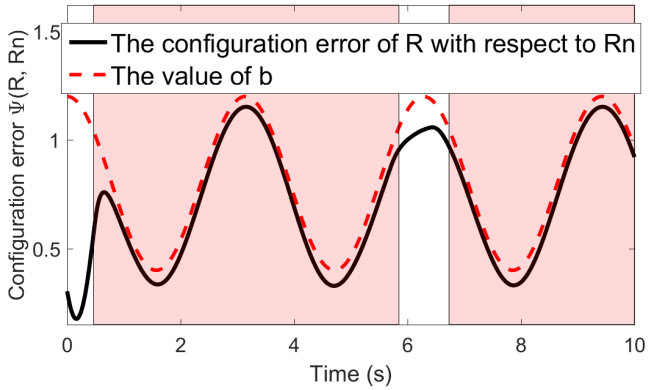

(a) Plot illustrating the configuration error $\Psi(R(t), R_n(t)) \leq b(t)$.

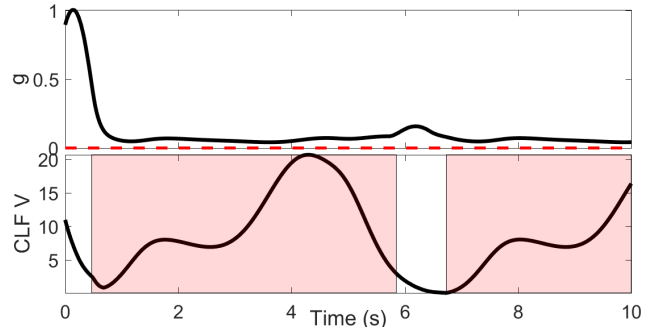

(b) Plots of the constraint function g and the geometric CLF V. The proposed controller ensures $g \geq 0$.

Fig. 12: *(3D Pendulum with Time-Varying Safety Constraints)*: Plots of configuration error, safety constraing, and geometric Lyapunov function. Durations when the reference is unsafe are highlighted in red.

VII. Conclusion and Future Work

We have considered the problem of safety-critical control of fully actuated simple mechanical systems. By extending the concepts of CLFs and CBFs to the configuration space of simple mechanical systems, we are able to develop the concepts of geometric CLFs and CBFs, which are coordinate free, and thus don't depend on the choice of local coordinates. A geometric CLF expression is given based on well-developed geometric control theory. We also propose a general method for constructing geometric CBFs, based on constraints given only in terms of configuration errors on various manifolds. Based on these CLF and CBF candidates, a CBF-CLF-QP controller is proposed to mediate between stability and safety. We have verified its performance both theoretically and based on several simulation tests on simple mechanical systems on $\mathbb{R}^3, \mathbb{S}^2$, and $SO(3)$.

Appendix

A. Proof of Lemma 1

From condition (8) and Chain rule, the time derivative of B could be expressed as:

$$\dot{B} = B'(h) \cdot \dot{h} \leq \frac{\mu}{B}$$

Hence, by Lemma. 1 in [3], the set $\{(q, \dot{q}) \in TM : B(t, q, \dot{q}) > 0\}$ is forward invariant, which is C_t° by the first condition of CBF.

B. Proof of Lemma 2

We will first select the candidate function to be $\beta(x) = x$ and choose any parameters γ_i such that $\gamma_i \geq c_i$ for $i = 1, 2, \cdots, k$. Then a candidate $\mathcal{C}_t$ is constructed.

Expanding out the expression of each h_i yields

$$h_i = (-1)^{\delta_i}(\dot{b}_i - \langle d_1 \Psi_{q,q_i}, \dot{q}\rangle - \langle d_2 \Psi_{q,q_i}, \dot{q}_i\rangle) + \gamma_i g_i$$

where the first bracket is evaluated at q, and the second is evaluated at q_i. Plugging in the property of transport map in (2), we have

$$h_i = (-1)^{\delta_i+1}\langle d\Psi_{q,q_i}, \dot{q} - \mathscr{T}_{q,q_i}\dot{q}_i\rangle + \gamma_i g_i + (-1)^{\delta_i}\dot{b}_i$$

Fix a time $t \geq 0$, since $\mathcal{B}_t$ is nonempty, it must contain a particular point $q \in \mathcal{B}_t$. Then for each $q \in \mathcal{B}_t$, if we want to find a tangent vector $\dot{q} \in T_qM$ such that $(q, \dot{q}) \in \mathcal{C}_t$, it must satisfy the conditions below for each $i = 1, 2, \cdots, k$:

$$(-1)^{\delta_i+1}\langle d\Psi_{q,q_i}, \dot{q} - \mathscr{T}_{q,q_i}\dot{q}_i\rangle + \gamma_i g_i + (-1)^{\delta_i}\dot{b}_i \geq 0 \qquad (31)$$

From the condition given, it holds that $\gamma_i g_i \geq c_i g_i \geq |\dot{b}_i| \geq -(-1)^{\delta_i}\dot{b}_i$, which implies $\gamma_i g_i + (-1)^{\delta_i}\dot{b}_i \geq 0$. Hence, by inspecting Eq. (31), we have $(q, \mathscr{T}_{q,q_i}\dot{q}_i) \in \mathcal{C}_t$ for each $q \in \mathcal{B}_t$ which makes $\mathcal{C}_t$ nonempty.

C. Proof of Lemma 3

Note that a set is path connected if every set of points in the set are connected by a piecewise continuously differentiable trajectory. To prove path connectedness of $\mathcal{C}_t^B$, we construct a path between any two points in $\mathcal{C}_t^B$ using geodesics and path-connectedness of $\mathcal{B}_t^\circ$. In particular, we want to propagate the initial state and the end state through geodesic flows and connect the geodesics together through the path connectedness of $\mathcal{B}_t^\circ$.

Given two states $(q, \dot{q}), (\hat{q}, \dot{\hat{q}}) \in \mathcal{C}_t^B$. We want to construct a piecewise smooth path $\Phi : [-1, 1] \to \mathcal{C}_t^B$ such that $\Phi(-1) = (q, \dot{q})$, $\Phi(1) = (\hat{q}, \dot{\hat{q}})$. Since the constraint function g_i is time-invariant, for any pair $(q, \dot{q}) \in \mathcal{C}_t^B$, it holds that

$$h_i = (-1)^{\delta_i+1}\langle d\Psi_{q,q_i}, \dot{q}\rangle + \gamma_i g_i > 0, \qquad (32)$$

For the case when $q = \hat{q}$, we know that both $\dot{q}, \dot{\hat{q}}$ belong to the same tangent space T_qM, which satisfy the condition (32). Since T_qM is a Hilbert space equipped with the Riemannian metric, the collection of tangent vectors satisfying (32) is an open convex polygon. Thus a straight line can connect them together as $\Phi(t) = \left(q, \frac{1}{2}(t\dot{q} + (1-t)\dot{\hat{q}})\right)$ where $t \in [-1, 1]$.

For the case when $q \neq \hat{q}$, a candidate path can be constructed in the following two steps. Since both $q, \hat{q} \in \mathcal{B}_t^\circ$, there exist two open neighborhoods U_1, U_2 around $q, \hat{q}$ such that $U_1, U_2 \subset \mathcal{B}_t^\circ$. Using the fact that M is a Riemannian manifold, there exists a unique geodesics passing through q, denoted as $\varphi_1 : [-1, 1] \to M$, which satisfies that $\varphi_1(0) = q,\ \varphi_1'(0) = \dot{q}$. Similarly, there's another geodesics $\varphi_2 : [-1, 1] \to M$ passing through $\hat{q}$ which satisfies $\varphi_2(0) = \hat{q},\ \varphi_2'(0) = \dot{\hat{q}}$. Also, since both U_1, U_2 are both nonempty open sets, they both contain closed subsets. Hence, there exist $\delta_1, \delta_2 > 0$ such that $\varphi_1([-\delta_1, \delta_1]) \subset U_1,\ \varphi_2([-\delta_2, \delta_2]) \subset U_2$. Considering the segments of geodesics $\varphi_1([-\delta_1, \delta_1]), \varphi_2([-\delta_2, \delta_2]) \subset \mathcal{B}_t^\circ$, we want to truncate these two geodesics to make sure the truncated parts with their derivatives are also contained in $\mathcal{C}_t^B$. Let $T_1 = \sup_{0 \le s \le \delta_1} \{h_i(\varphi_1(s), \varphi_1'(s)) > 0$ for every $i = 1, 2, \cdots, k\}$, $T_2 = \inf_{-\delta_2 \le s \le 0} \{h_i(\varphi_2(s), \varphi_2'(s)) > 0$ for every $i = 1, 2, \cdots, k\}$. Since the functions $h_i(\varphi_1(s), \varphi_1'(s))$ are smooth functions defined on $[-\delta_1, \delta_1]$, then it holds that $T_1 > 0$. Or otherwise, for each i, we could find a sequence $\{t_n\} \to 0$ such that $h_i(\varphi_1(t_n), \varphi_1'(t_n)) = 0$ which would imply that $h_i(q, \dot{q}) = 0$. This leads to a contradiction and that $T_1 > 0$. Applying a similar argument to φ_2 yields that $T_2 < 0$. Also, by the definition of T_1, T_2, we have the subset $\{(\varphi_1(t), \varphi_1'(t)) \in TM : 0 \le t \le T_1/2\},\ \{(\varphi_2(t), \varphi_2'(t)) \in TM : T_2/2 \le t \le 0\} \subset \mathcal{C}_t^B$. Since both $\varphi_1(T_1/2), \varphi_2(T_2/2) \in \mathcal{B}_t^\circ$, using the path connectedness of $\mathcal{B}_t^\circ$, there exists a piecewise smooth path $\varphi_3 : [-1, 1] \to \mathcal{B}_t^\circ$ which satisfies $\varphi_3(-1) = \varphi_1(T_1/2),\ \varphi_3(1) = \varphi_2(T_2/2)$.

The next step is to scale the path φ_3 to make sure its derivative satisfies the condition (32) all the time. Define a new path as $\psi(t) = \varphi_3(t/K)$ whose derivative is given by $\psi'(t) = \varphi_3'(t/K)/K$ where $K > 0$. Note that for the scaled trajectory ψ, it is defined on $[-K, K]$. In order to make sure $(\psi(t), \psi'(t)) \in \mathcal{C}_t^B$ for every $t \in [-K, K]$, the following inequality should hold

$$\frac{1}{K}(-1)^{\delta_i+1}\langle d\Psi_{\varphi_3(t/K), q_i}, \varphi_3'(t/K)\rangle + \gamma_i g_i(\varphi_3(t/K)) > 0$$

which can be converted to the inequality below,

$$K \ge \frac{(-1)^{\delta_i}\langle d\Psi_{\varphi_3(u), q_i}, \varphi_3'(u)\rangle}{\gamma_i g_i(\varphi_3(u))} = s_i(u) \tag{33}$$

for every $i = 1, 2, \cdots, k$ and every $u \in [-1, 1]$.

Since $\varphi_3(u) \in \mathcal{B}_t^\circ$, by definition $g_i(\varphi_3(u)) > 0$ for every $u \in [-1, 1]$. Hence, function $s_i(u)$ on the right hand side of (33) is well-defined and piecewise continuous over the interval $[-1, 1]$. Because there are only finite jumps of s_i in the whole interval $[-1, 1]$, it has a maximum value over the compact interval $[-1, 1]$ for each i. Let $K_0 = \max_{i=1,2,\cdots,k} \sup_{u \in [-1,1]} s_i(u)$ which is finite. Then, pick a value $K > K_0$ and we could make sure that $(\psi(t), \psi'(t)) \in \mathcal{C}_t^B$ for all $t \in [-K, K]$.

Now assemble the final path together as $\Phi(t) = (\varphi_1(t), \varphi_1'(t))$ when $0 \le t \le \frac{T_1}{2}$; $\Phi(t) = (\varphi_1(\frac{T_1}{2}), \frac{2(T_1 - t)}{T_1}\varphi_1'(\frac{T_1}{2}) + \frac{2t - T_1}{T_1}\psi'(-K))$ when $\frac{T_1}{2} \le t \le T_1$; $\Phi(t) = (\psi(t - T_1), \psi'(t - T_1))$ when $T_1 \le t \le T_1 + 2K$; $\Phi(t) = (\varphi_2(\frac{T_2}{2}), \frac{2(T_1 + 2K - T_2/2 - t)}{-T_2}\psi'(K) + \frac{2(T_1 + 2K - t)}{T_2}\varphi_2'(\frac{T_2}{2}))$ when $T_1 + 2K \le t \le T_1 + 2K - T_2/2$; $\Phi(t) = (\varphi_2(t + T_2 - T_1 - 2K), \varphi_2'(t + T_2 - T_1 - 2K))$ when $T_1 + 2K - T_2/2 \le t \le T_1 + 2K - T_2$. Note from the construction, the overall trajectory $\Phi(t)$ is continuous and piecewise smooth. Also, using the properties of $\varphi_1, \varphi_2, \psi$, it holds that $\Phi([0, T_1 - T_2 + 2K]) \in \mathcal{C}_t^B$ which connects any pair of $(q, \dot{q}), (\hat{q}, \dot{\hat{q}})$. Thus, the set $\mathcal{C}_t^B$ is path connected.

D. Proof of Proposition 1

Since $(q_0, \dot{q}_0) \in \mathcal{C}_0$, by forward invariance, it holds that $(q(t), \dot{q}(t)) \in \mathcal{C}_t$ which is equivalent to

$$\gamma_i \beta(g_i(q(t))) + \langle dg_i, \dot{q}(t)\rangle + \frac{\partial g_i}{\partial t}|_{t, q(t)} \ge 0 \tag{34}$$

for any $i \in \{1, 2, \cdots, k\}$ and $t \in [0, \infty)$

Consider the extreme case when the system trajectory reaches the boundary of $\mathcal{B}_t$ at $t_1 > 0$, then there exists $j \in \{1, 2, \cdots, k\}$ such that $g_j(t_1, t_1, q(t_1)) = 0$. By Chain rule and the previous inequality (34), it follows that

$$\left.\frac{dg_j}{dt}\right|_{t=t_1} = \langle dg_j, \dot{q}(t_1)\rangle + \frac{\partial g_j}{\partial t}|_{t_1, q(t_1)} \ge 0,$$

which means that the value of g_j would never decrease below zeros.

The previous argument indicates that the system trajectory would never escape $\mathcal{B}_{j,t}$ when it reaches the boundary of $\mathcal{B}_{i,t}$. This implies that the system trajectory would never escape the safety region $\mathcal{B}_t$, namely, $\mathcal{B}_t$ is forward invariant.

E. Proof of Proposition 2

Consider the quadratic programming in (20) with positive definite coefficient matrix $Q > 0$. Then if a solution exists for this QP which is strictly convex, this solution is unique according to proposition in convex optimization. So by assumption this control input is well-defined.

Since the set $\mathcal{D}$ has measure zero, it has an empty interior. Hence, the system's trajectory can only traverse it at discrete time points. For the time period (t_1, t_2) when $(q, \dot{q}) \in \mathcal{C} \backslash \mathcal{D}$, all the hard constraints are satisfied by the controller. Applying Theorem 2 in [3] yields that system trajectory would never escape $\mathcal{C} \backslash \mathcal{D}$. When $(q, \dot{q}) \in \mathcal{D}$, a solution might not exist but the current state lies in C° since $\mathcal{D} \in C^\circ$. For both cases, the system state always stay within $\mathcal{C}$. Thus it's forward-invariant for system (3). Using Proposition (1), it follows that the feasible region $\mathcal{B}$ is also forward-invariant.

REFERENCES

[1] M. Althoff, O. Stursberg, and M. Buss, "Reachability analysis of nonlinear systems with uncertain parameters using conservative linearization," *IEEE Conference on Decision and Control*, 2008.

[2] A. D. Ames, K. Galloway, K. Sreenath, and J. W. Grizzle, "Rapidly exponentially stabilizing control lyapunov functions and hybrid zero dynamics," *IEEE Transactions on Automatic Control (TAC)*, vol. 59, no. 4, pp. 876–891, Apr. 2014.

[3] A. Ames, J. Grizzle, and P. Tabuada, "Control barrier function based quadratic programs with application to adaptive cruise control," in *IEEE Conference on Decision and Control*, 2014.

[4] E. Asarin, O. Bournez, T. Dang, and O. Maler, "Approximate Reachability Analysis of Piecewise-Linear Dynamical Systems," *Lecture Notes in Computer Science, Hybrid Systems: Computation and Control*, vol. 1790, pp. 20–31, 2000.

[5] A. Bemporad, "Reference governor for constrained nonlinear systems," *IEEE Transactions on Automatic Control*, vol. 43, no. 3, pp. 415–419, March 1998.

[6] F. Bullo and A. Lewis, *Geometric Control of Mechanical Systems*, ser. Texts in Applied Mathematics. Springer Verlag, 2004, vol. 49.

[7] F. Bullo and R. M. Murray, "Tracking for fully actuated mechanical systems: a geometric framework," *Automatica*, vol. 35, no. 1, pp. 17–34, Jan. 1999.

[8] N. A. Chaturvedi, A. K. Sanyal, and N. H. McClamroch, "Rigid-body attitude control," *IEEE Control Systems Magazine*, vol. 31, no. 3, pp. 30–51, June 2011.

[9] K. Galloway, K. Sreenath, A. D. Ames, and J. W. Grizzle, "Torque saturation in bipedal robotic walking through control lyapunov function based quadratic programs," *IEEE Access*, vol. 3, pp. 323–332, Apr. 2015.

[10] C. E. García, D. M. Prett, and M. Morari, "Model Predictive Control: Theory and Practice - A Survey," *Automatica*, vol. 25, no. 3, pp. 335–348, 1989.

[11] V. Guillemin and A. Pollack, *Differential Topology*. AMS Chelsea Publishing, 1974.

[12] R. Gupta, U. V. Kalabic, S. D. Cairano, A. M. Bloch, and I. V. Kolmanovsky, "Constrained spacecraft attitude control on so(3) using fast nonlinear model predictive control," in *American Control Conference*, 2015, pp. 2980–2986.

[13] A. Jadbabaie and J. Hauser, "On the stability of receding horizon control with a general terminal cost," *IEEE Trans. on automatic control*, vol. 50, no. 5, pp. 674–678, 2005.

[14] U. Kalabic, I. V. Kolmanovsky, and E. G. Gilbert, "Reduced order extended command governor," *Automatica*, vol. 50, no. 5, pp. 1466–1472, 2014.

[15] U. V. Kalabic, R. Gupta, S. D. Cairano, A. M. Bloch, and I. V. Kolmanovsky, "Constrained spacecraft attitude control on so(3) using reference governors and nonlinear model predictive control," in *American Control Conference*, Portland, Oregon, 2014, pp. 5586–5593.

[16] Y. Kim and M. Mesbahi, "Quadratically Constrained Attitude Control via Semidefinite Programming," *IEEE Transactions on Automatic Control*, vol. 49, no. 5, pp. 731–735, May 2004.

[17] Y. Kim, M. Mesbahi, G. Singh, and F. Y. Hadaegh, "On the Convex Parameterization of Constrained Spacecraft Reorientation," *IEEE Trans. Aerosp. Electron. Syst.*, vol. 46, no. 3, pp. 1097–1109, Jul. 2010.

[18] T. Lee, M. Leok, and N. H. McClamroch, "Stable manifolds of saddle equilibria for pendulum dynamics on S^2 and SO(3)," *IEEE Conf. on Decision and Control*, pp. 3915–3921, Dec. 2011.

[19] T. Lee, M. Leoky, and N. McClamroch, "Geometric tracking control of a quadrotor UAV on SE (3)," *IEEE Conference on Decision and Control*, pp. 5420–5425, 2010.

[20] T. Lee, K. Sreenath, and V. Kumar, "Geometric control of cooperating multiple quadrotor UAVs with a suspended payload," in *IEEE Conf. on Decision and Control*, Dec. 2013, pp. 5510–5515.

[21] U. Lee and M. Mesbahi, "Spacecraft reorientation in presence of attitude constraints vs logarithmic barrier potentials," in *American Control Conference*, San Francisco, June 2011.

[22] J. Lygeros, G. Pappas, and S. Sastry, "An introduction to hybrid systems modeling, analysis and control," in *In Preprints of the First Nonlinear Control Network Pedagogical School*, 1999, pp. 307–329.

[23] D. Mayne, J. Rawlings, C. Rao, and P. Scokaert, "Constrained model predictive control: Stability and optimality," *Automatica*, vol. 36, no. 6, pp. 789–814, 2000.

[24] I. Mitchell, a. Bayen, and C. Tomlin, "A time-dependent Hamilton-Jacobi formulation of reachable sets for continuous dynamic games," *IEEE Transactions on automatic control*, vol. 50, pp. 947–957, 2005.

[25] F. Morgan, *Geometric measure theory: a beginner's guide*. Academic press, 2008.

[26] B. Morris, M. J. Powell, and A. D. Ames, "Sufficient conditions for the Lipschitz continuity of QP-based multi-objective control of humanoid robots," *IEEE Conf. on Decision and Control*, pp. 2920–2926, 2013.

[27] S. Prajna and A. Jadbabaie, "Safety verification of hybrid systems using barrier certificates," in *Hybrid Systems: Computation and Control*, 2004.

[28] M. Z. Romdlony and B. Jayawardhana, "Stabilization with guaranteed safety using control lyapunov-barrier function," *Automatica*, vol. 66, pp. 39–47, 2016.

[29] E. Sontag and H. J. Sussmann, "Nonsmooth control-lyapunov functions," in *IEEE Conf. on Decision and Control*, vol. 3. IEEE, 1995, pp. 2799–2805.

[30] K. Sreenath, T. Lee, and V. Kumar, "Geometric control and differential flatness of a quadrotor UAV with a cable-suspended load," in *IEEE Conf. on Decision and Control*, Dec. 2013, pp. 2269–2274.

[31] K. P. Tee and S. S. Ge, "Control of nonlinear systems with full state constraint using a Barrier Lyapunov Function," *IEEE Conference on Decision and Control*, pp. 8618–8623, Dec. 2009.

[32] K. P. Tee, S. S. Ge, and E. H. Tay, "Barrier Lyapunov Functions for the control of output-constrained nonlinear systems," *Automatica*, vol. 45, no. 4, pp. 918–927, Apr. 2009.

[33] Y. Wang and S. Boyd, "Fast model predictive control using online optimization," *Control Systems Technology, IEEE Transactions on*, vol. 18, no. 2, pp. 267–278, 2010.

[34] A. Weiss, F. Leve, M. Baldwin, J. Forbes, and I. Kolmanovsky, "Spacecraft constrained attitude control using positively invariant sets on $so(3) \times r^3$," in *American Control Conference*, 2014, pp. 4955–4960.

[35] P. Wieland and F. Allgower, "Constructive safety using control barrier functions," in *Nonlinear Control Syst.*, vol. 7, no. 1, 2007, pp. 462–467.

[36] A. G. Wills and W. P. Heath, "Barrier function based model predictive control," *Automatica*, vol. 40, no. 8, pp. 1415–1422, Aug. 2004.

[37] R. Wisniewski and C. Sloth, "Converse barrier certificate theorem," in *IEEE Conference on Decision and Control*, 2013.

[38] G. Wu and K. Sreenath, "Safety-critical and constrained geometric control synthesis using control lyapunov and control barrier functions for systems evolving on manifolds," in *American Control Conference*, Jul. 2015, pp. 2038–2044.

[39] X. Xu, P. Tabuada, J. W. Grizzle, and A. D. Ames, "Robustness of control barrier functions for safety critical control," in *Analysis and Design of Hybrid Systems*, Atlanta, GA, October 2015, pp. 54–61.

PLACE PHOTO HERE

Guofan Wu Guofan Wu is a PhD candidate in Mechanical Engineering at Carnegie Mellon University. His research interest is focused on nonlinear control theory, especially geometric control methods with application to quadrotor control.

PLACE PHOTO HERE

Koushil Sreenath Koushil Sreenath is an Assistant Professor of Mechanical Engineering, Robotics Institute, and Electrical & Computer Engineering, Carnegie Mellon University. He received the Ph.D. degree in Electrical Engineering: Systems and the M.S. degree in Applied Mathematics from the University of Michigan at Ann Arbor, MI, in 2011. His research interest lies at the intersection of highly dynamic robotics and applied nonlinear control. He received the best paper award in RSS 2013, and the Google Faculty Research Award in Robotics in 2015.